Journal Pre-proofs

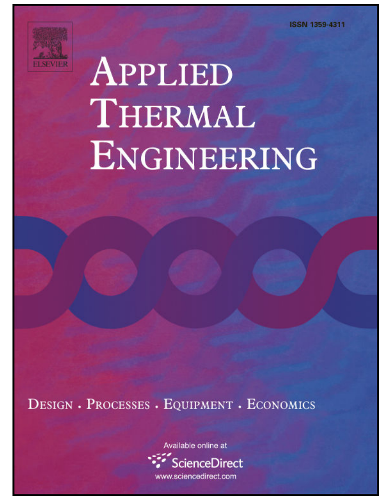

Experimental and Numerical Analysis of a New Modification for Enhancing Thermal Performance of a Shell and Helically Coiled Heat Exchanger

Azim Doğuş Tuncer, Adnan Sözen, Ataollah Khanlari, Emine Yağ ız Gürbüzb, Halil İbrahim Variyenli

PII:	S1359-4311(20)33751-0
DOI:	https://doi.org/10.1016/j.applthermaleng.2020.116272
Reference:	ATE 116272

To appear in: *Applied Thermal Engineering*

Received Date:	8 June 2020
Revised Date:	17 October 2020
Accepted Date:	25 October 2020

Please cite this article as: A. Doğuş Tuncer, A. Sözen, A. Khanlari, E. Yağ ız Gürbüzb, H. İbrahim Variyenli, Experimental and Numerical Analysis of a New Modification for Enhancing Thermal Performance of a Shell and Helically Coiled Heat Exchanger, *Applied Thermal Engineering* (2020), doi: https://doi.org/10.1016/j.applthermaleng.2020.116272

Experimental and Numerical Analysis of a New Modification for Enhancing Thermal Performance of a Shell and Helically Coiled Heat Exchanger

Azim Doğuş Tuncer[1,2], Adnan Sözen[3], Ataollah Khanlari[4,*], Emine Yağız Gürbüz[2,5], Halil İbrahim Variyenli[3]

[1]Energy Systems Engineering, Burdur Mehmet Akif Ersoy University, Burdur, Turkey

[2]Natural and Applied Science Institute, Gazi University, Ankara, Turkey

[3]Energy Systems Engineering, Gazi University, Ankara, Turkey

[4]Mechanical Engineering, University of Turkish Aeronautical Association, Ankara, Turkey

[5]Energy Systems Engineering, Muğla Sıtkı Koçman University, Muğla, Turkey

Abstract

Shell and helically coiled tube heat exchangers composed from curved tubes inside a shell which are often preferred devices particularly in several applications like refrigeration, heat recovery systems, chemical processing, heat storage and food processing. Enhancing the effectiveness of heat exchangers can leads to increase in the overall efficiency of energy conversion systems. In addition, finding a simple and cost-effective method for enhancing the effectiveness of heat exchangers is a significant issue that should be taken into consideration. In this work, it is proposed to enhance the performance of a shell and helically coiled heat exchanger by utilizing a new modification. Within this context, a hollow tube integrated into the shell side and cold fluid enters the heat exchanger along this tube. The main purpose of this modification is regulating the fluid flow over the helically coiled tube and consequently obtaining more thermal energy. In this regard, the performance of a modified shell and helically coiled heat exchanger has been compared with a conventional vertical shell and helically coiled heat exchanger by using numerical simulation. The main objective of the simulation part of this study is determining suitable configuration for shell and helically coiled tube heat exchanger to obtain high thermal performance. Then, modified shell and helically coiled heat exchanger has been fabricated by considering simulation results. Finally, the performance analysis of developed heat exchanger has been experimentally conducted under different conditions to determine its behavior. The findings of this work showed the successful design of the modified heat exchanger. Generally, it can be said that integrating a hollow tube into the shell side of the heat exchanger led to regulate the fluid flow in the shell side that improved heat transfer. Overall heat transfer coefficient obtained in the range of 1600-3150 W/m^{2}K. Also, heat transfer coefficient of coil side in this study was obtained in the range of 5700-13400 W/m^{2}K. Moreover, average difference between simulation and experimental results is 8%.

Keywords: Heat exchanger; helically coiled; performance enhancement; simulation; experimental

Nomenclature

A	heat transfer area (m^2)
c_p	specific heat capacity (kJ/kg.K)
C	heat capacity rate (W/K)
d	coiled tube diameter (m)
d_{inner}	inner diameter of coiled tube (m)
D_{coil}	coil diameter (m)
D_{shell}	shell diameter (m)
D_h	hydraulic diameter
De	Dean Number
E	total energy (J)
H	height
h	heat transfer coefficient (W/m^2.K)
k	thermal conductivity (W/m.K)
$\dot{m}$	mass flow rate (kg/s)

Nu	Nusselt Number
p	pressure (Pa)
Pr	Prandtl Number
Re	Reynolds Number
T	temperature (K)
$\dot{Q}$	heat transfer rate (W)
U	overall heat transfer coefficient (W/m^2.K)
V	velocity (m/s)
$\vec{v}$	overall velocity vector (m/s)
w_1,w_2,w_n	the uncertainties in the independent variables
W_R	the total uncertainty (%)
Greek letters	
ΔT_{LMTD}	logarithmic mean temperature difference (K)
ε	effectiveness
μ	dynamic viscosity (Pa.s)
ρ	density (kg/m^3)
Subcripts	
c	coil
in	inlet
it	inner tube
out	outlet
t	tube

1. Introduction

Increasing energy consumption and limited fossil fuel reserves have been led to look for new energy resources and energy systems. Also, available energy sources must be used efficiently. Thus, new studies are ongoing for enhancing existing energy conversion technologies and developing new systems. Heat exchangers (HEs) are devices that used in various applications such as cooling, heating and other energy conversion systems that many studies have been permanently performed in order to enhance their thermal efficiency. Shell and helically coiled tube HEs composed from curved tubes inside a shell which are often preferred devices particularly in industry and several applications like refrigeration, heat recovery systems, chemical processing, heat storage and food processing [1]. Furthermore, they are mostly used in petroleum units in order to reduce the temperature of lubricating oil which is used in the pumps and in double pipe HEs [2-4]. In this type of HEs, working fluid flows over the curved tubes lead to creating centrifugal force. The generated centrifugal force has a notable impact on flow behavior in the HE. The heat transfer rate and pressure drop for flow in helically coiled tube HEs are higher than that of the straight tubes. However, utilizing helically coiled tube instead of ordinary straight tube cause to enhance heat transfer rate because the heat transfer area increases by using helically coiled tube.

Numerous studies are available in the literature which investigated shell and helically coiled HEs [5-6]. Jamshidi et al. [7] conducted an experimental work on a shell and helically coiled tube HE in order to enhance the rate of heat transfer. They investigated flow parameters and geometrical factors like coil pitch and coil diameter in the laminar flow regime. In another experimental work done by Hardik et al. [8] the influences of the tube curvature on heat transfer and flow behavior analyzed. Sadighi Dizaji et al. [9] analyzed the influences of flow and geometrical parameters on the performance of a shell and helically coiled HE by using exergy methodology. Ramesh et al. [10] experimentally studied a shell and helically coiled HE in the vapor absorption refrigeration system. Andrzejczyk and Muszynski [11] investigated the influence of utilizing continuous core-baffle geometry on heat transfer enhancement in a shell and helically coiled HE. Khorasani et al. [12] experimentally analyzed the impact of air injection on the thermal efficiency of a shell and helically coiled HE. Kannadasan et al. [13] utilized CuO/water nanofluid to increase the performance of a shell and helically coiled HE. Andrzejczyk et al. [14] experimentally analyzed the effects of adding various baffles on efficiency increment in a helically coiled HE. Khorasani and Dadvand [15] studied the influence of air bubble injection on the effectiveness of a horizontalshell and helically coiled HE. Miansari et al. [16] analyzed a shell and helically coiled HE by using energy-exergy methodology. Solanki and Kumar [17] experimentally studied heat transfer and pressure drop in a shell and helically coiled HE using R-134a as working fluid. Rahimi et al. [18] analyzed the influence of coil diameter on the thermal performance of a shell and helically coiled HE. Alimoradi and Veysi [19] determined optimal and critical values of geometrical parameters for a shell and helically coiled HE.

In addition to the experimental works, there are a lot of studies are available in the literature which utilized numerical methods to investigate different types of HEs [20-23]. As it is known experimental works are expensive and time-consuming. Therefore, numerical methods can be employed to analyze the effects of various factors on the performance of HEs without any payment for the experimental apparatus. Mirgolbabaei [24] utilized Ansys Fluent to model a helically coiled HE at various mass flow rates of shell side and various geometrical configurations. Cancan et al. [25] numerically studied the impact of adding spherical corrugation in a helically coiled tube in tube HE. Omidi et al. [26] simulated a helically coiled tube HE with lobed cross sections to determine the impact of various geometrical factors. Etghani and Hosseini Baboli [27] used CFD approach to simulate a shell and helically coiled HE and analyzed the effects of factors like coil pitch, tube diameter and flow rate on HE's performance. Chen et al. [28] numerically investigated the effect of adding fins on coiled tube of a shell and helically coiled HE with the aim of enhancing the overall efficiency. Wang et al. [29] developed and analyzed thermohydraulic performance of a shell and helically twisted-coiled HE and stated that utilizing twisted-coiled can improve the performance notably. Wu et al. [30] proposed a shell and helically coiled HE to be utilized in magnesium-based metal hydride reactor. Mangrulkar et al. [31] experimentally and numerically analyzed the performance of a cross-flow HE utilizing elliptical tubes. Wang et al. [32] numerically analyzed heat and flow characteristics of a shell and helically coiled trilobal HE and verified by experimental data. In another study, Wang et al. [33] conducted a comprehensive study on a shell and helically coiled HE to determine optimum working condition.

Some researchers tried to increase the performance of HE by extending the heat transfer surface area. In addition, integrating extended surfaces like fins to the HEs generate additional turbulence that increases the heat transfer rate [34, 35]. Kumar et al. [36] utilized perforated and solid circular fins and twisted tape insert with the aim of enhancing the performance of a tubular HE. Choudhary et al. [37] used a perforated splitter plate in a cross-flow tube bank to improve thermohydraulic performance. Bhattacharyya et al. [38] experimentally studied the influences of the inline and staggered angular cut baffle on the thermohydraulic characteristics of HE.

Researchers also indicated that increment of the heat transfer coefficient (HTC) of the inner side of the coiled tube was affected by three parameters namely increment of the inlet velocity, decrement of coil diameter and increment of the coil pitch [39-42].

Analyzing available studies in the literature indicated that various methods can be applied to increase the effectiveness of shell and helically coiled HEs. Adding various types of fins and baffles is widely used by many researchers to improve the performance of shell and helically coiled HEs. However, they indicated that using extended heat transfer surfaces can lead to increase pressure drop and fouling factor. The major objective of this work is to determine the appropriate configuration for helically coiled tube HE to achieve high thermal efficiency. In other words, it is proposed to upgrade the thermal performance of a shell and helically coiled HE by utilizing a new modification. In this regard, a hollow tube integrated into the shell side and cold fluid enters to the HE along this tube. The main purpose of this modification is regulating the fluid flow over the helically coiled tube and consequently obtaining more thermal energy. Firstly, the performance of modified shell and helically coiled HE in this study has been compared with a conventional vertical shell and helically coiled HE by using CFD approach. Then, modified shell and helically coiled HE has been fabricated by considering obtained numerical outcomes. Finally, the performance analysis of developed HE has been experimentally conducted to determine its behavior. Fig. 1 illustrates major structure of this study.

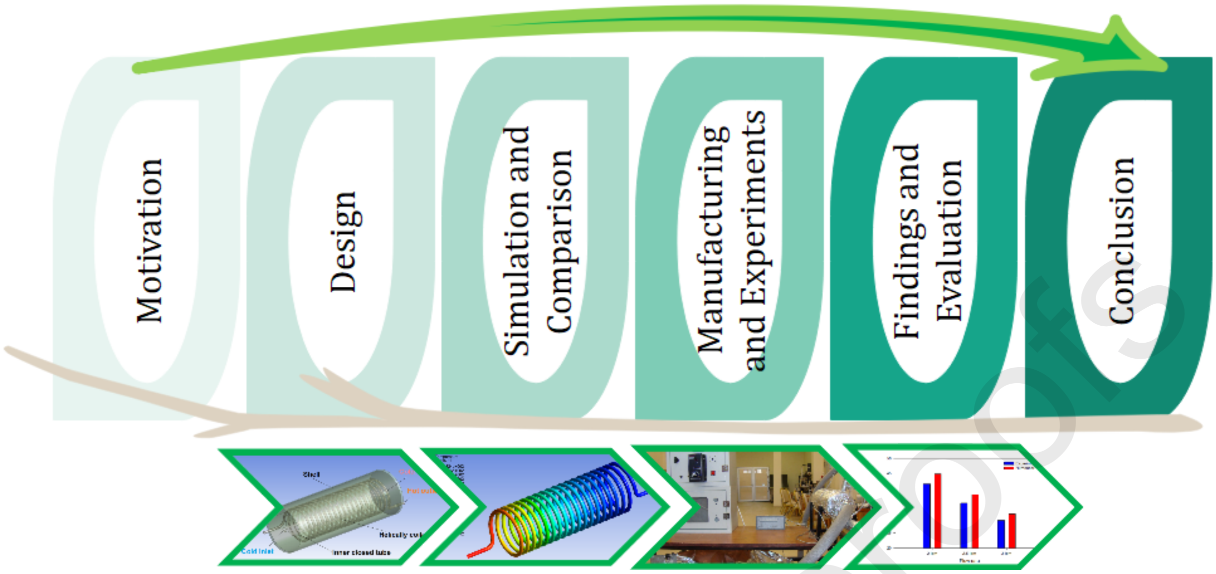

Fig. 1. Major structure of this study

2. Material and Method

2.1. CFD analysis

In this part, computational fluid dynamics (CFD) method has been utilized to simulate heat transfer and fluid flow inside the shell and helically coiled tube HE. The main objective of this simulation is to determine the suitable configuration for helically coiled tube HE to obtain high thermal efficiency. In this context, two different configurations for shell and helically coiled tube HEs have been designed regarding the previous studies. The geometry of designed HEs is given in Fig. 2. The first HE (Fig. 2a) is a vertical conventional type and has a closed tube in the middle of the HE with the aim of regulating fluid flow in the shell side and absorb more energy by cold fluid in the shell side. The first HE is oriented in the upright position and cold fluid enters the HE from the bottom side and it leaves from top side. The second HE has a different design and horizontally oriented. As can be seen in Fig. 2b, a hollow tube integrated in the shell side and cold fluid enters the HE along this tube. In other words, the cold fluid enters inner tube of the shell side, then it reaches the main shell part and flows over the helically coiled tube and finally leaves the HE as it can be seen in Fig. 2b. This modification can regulate the fluid flow in the shell side and improve thermal efficiency of HE. Detailed view of simulated

HEs is given in Fig. 3. In addition, a side view of HEs is illustrated in Fig. 4 that shows the flow pattern in two HEs. It is better to state that shell and helically coiled tube in both simulated HEs have the same dimensions. The coil has a diameter of D_{coil} and distance between two adjacent turns which is called pitch (p). A helically coiled tube is placed in the space among the shell and inner tube. Geometrical details of shell and helically coiled tube HEs is given in Table 1.

Generated mesh for numerical simulation is given in Fig. 5. It should be stated that finer meshes have been generated in the helically coiled tube and zones near the tube in the cold side and hot side to achieve more accurate findings. The mesh structure of the analyzed volume is a significant matter that affect the accuracy of the simulation. In the present research, mesh independency studies were conducted to achieve proper mesh for each HE. Table 2 demonstrates various mesh configurations for each HE. In this regard, different mesh combinations with various mesh numbers were generated to specify suitable mesh structure for each HE. Numerical analysis has been conducted by using each mesh for determining the proper mesh structure. Mesh D has been chosen to be used for all analyses because by rising mesh elements number, achieved outlet temperature was not changed. The quality of the composed mesh could be examined by utilizing various factors. Skewness value of designed mesh can be a good parameter in evaluating its quality. The maximum skewness value for conventional and modified HEs are 0.80 and 0.84, respectively. Moreover, the mean skewness value for conventional and modified HEs are 0.12 and 0.15, respectively.

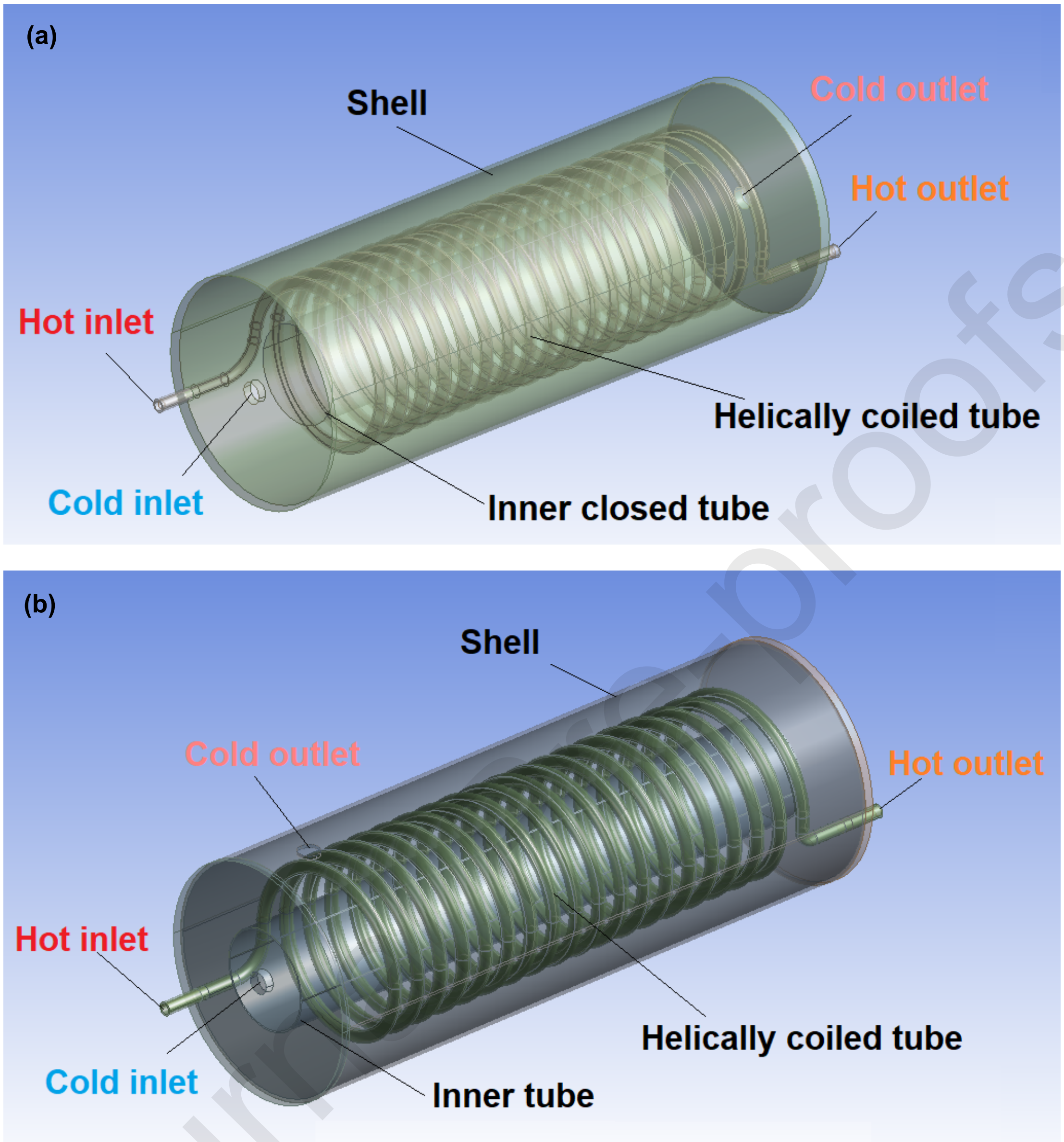

Fig. 2. Geometry of shell and helically coiled tube HEs a) Conventional type HE; b) Modified type HE

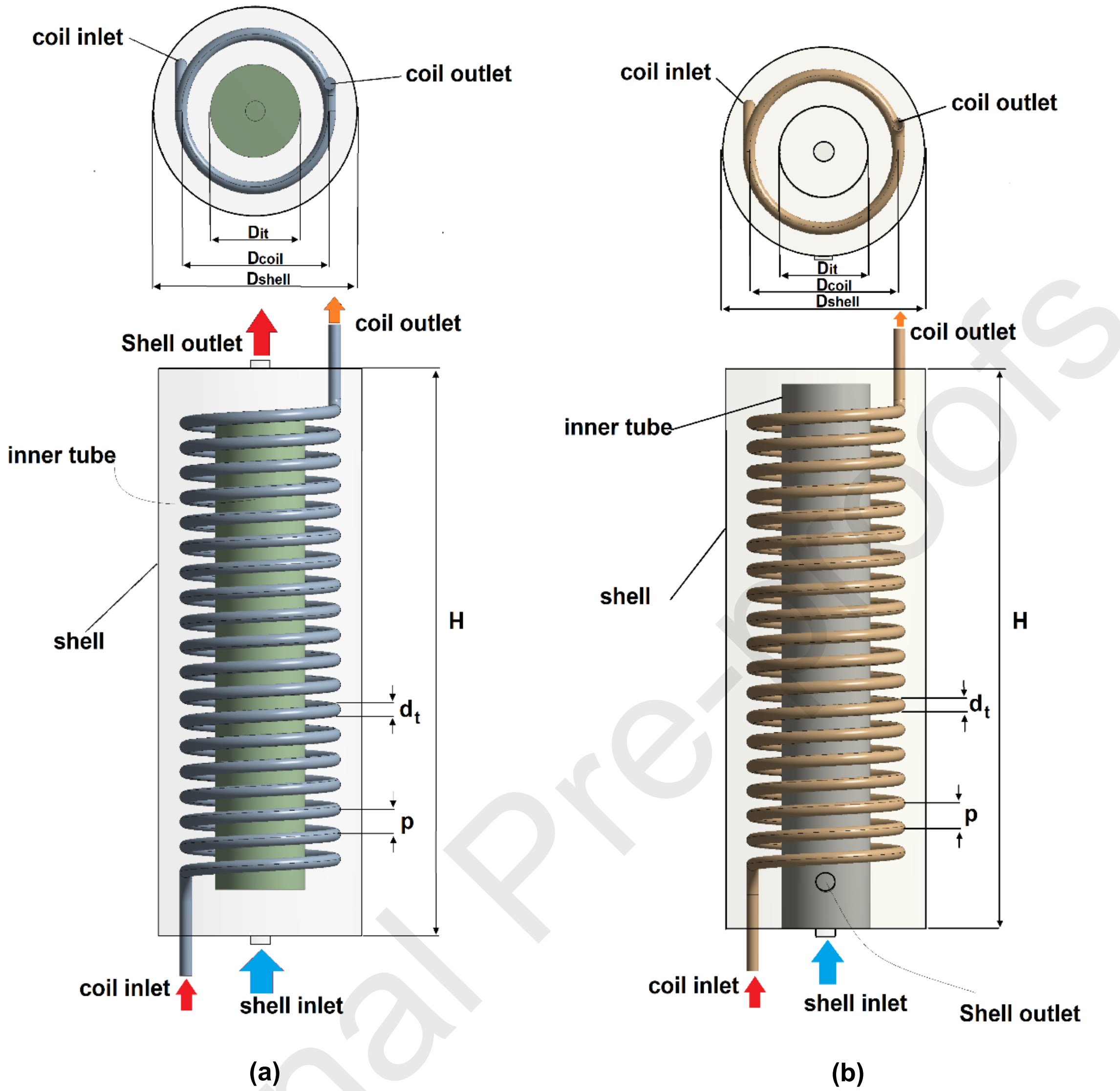

Fig. 3. Detailed view of simulated heat exchangers; a) Conventional type HE; b) Modified type HE

Table 1. Details of shell and helically coiled tube HE

	Conventional	**Modified**
Parameter	**Value**	**Value**
Interior diameter of coiled tube	0.006 m	0.006 m
Exterior diameter of coiled tube	0.008 m	0.008 m
Coil diameter	0.1 m	0.1 m
Coil pitch	0.016 m	0.016 m
Number of turns	18	18
Shell diameter	0.14 m	0.14 m
Shell height	0.375 m	0.375 m
Inner tube diameter	0.060 m	0.060 m
Inner tube height	0.305 m	0.325 m

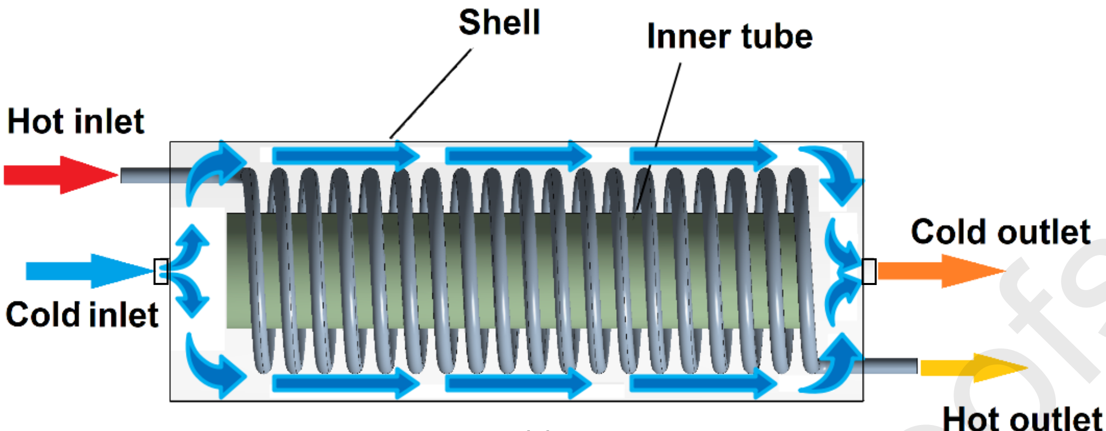

(a)

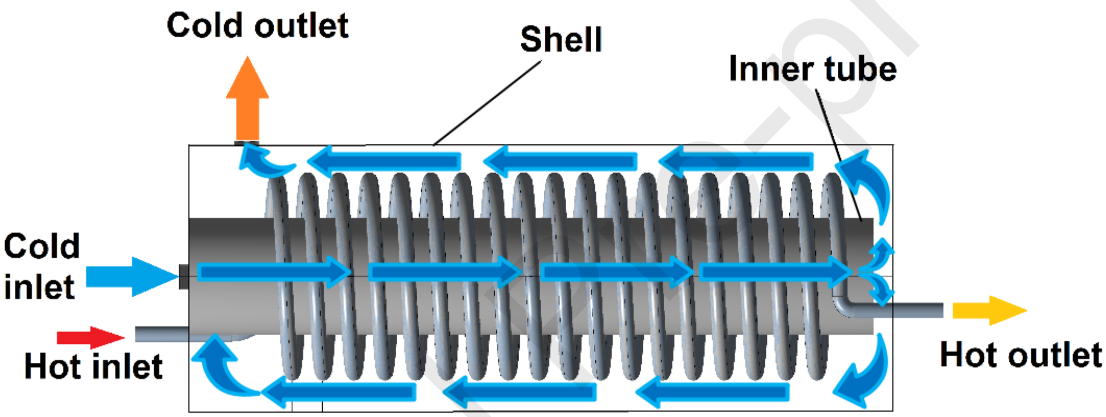

(b)

Fig. 4. A side view of HEs; a) Conventional type HE; b) Modified type HE

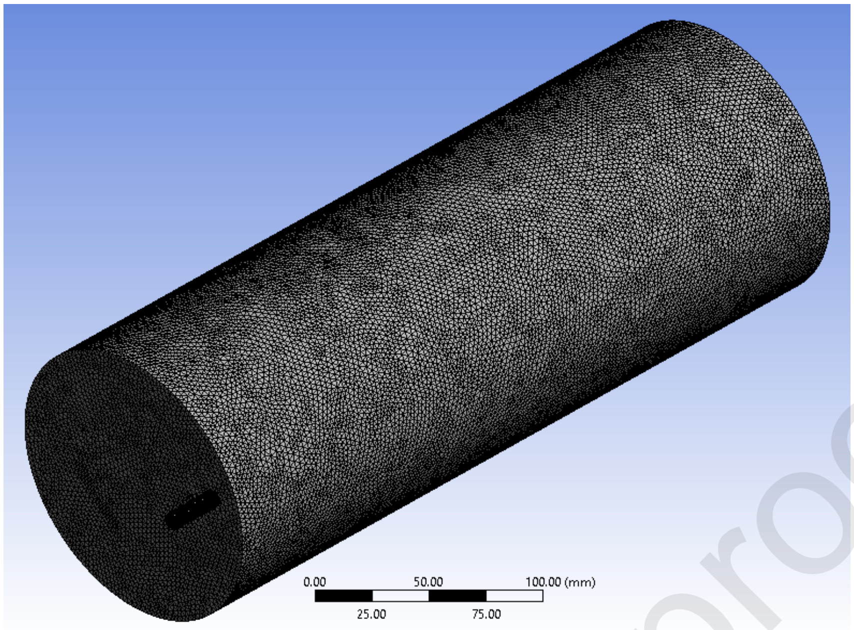

(a)

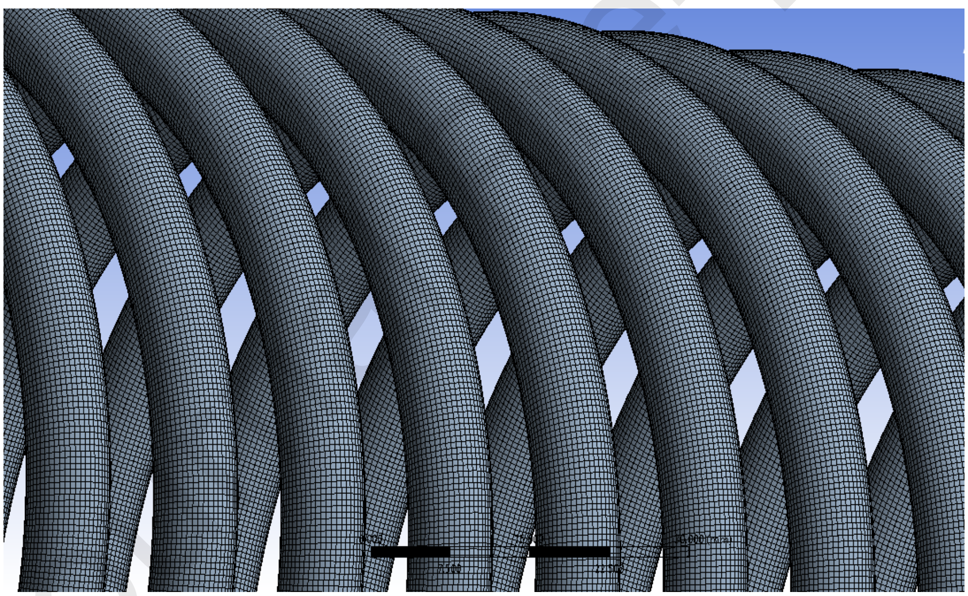

(b)

Fig. 5. Generated mesh for numerical simulation; a) Whole heat exchanger, b) Helically coiled tube

Table 2. Various meshes generated for HEs

Type	Mesh statistics	Mesh A	Mesh B	Mesh C	Mesh D
Conventional	Elements	2192617	4941608	8100947	10484487
	Nodes	491471	1662722	1610392	2628809
Modified	Elements	3540098	6104017	9366132	11934741
	Nodes	1373050	1821330	7368525	7817511

Shell and helically coiled tube HEs have been modeled by employing Fluent program to investigate thermal and flow characteristics of them. The governing equations utilized in the simulation of HEs consist of mass, momentum and energy conservation equations. In addition, a turbulent model must be selected to simulate flow inside the shell and helically coiled tube HEs. In this regard, different models have been tested considering related studies that investigated different HEs numerically [43-44]. Consequently, k-ε turbulence model (RNG) by adding enhanced wall functions was preferred to be used in the simulation of HEs. Numerical analysis of HEs has been conducted using a steady-state working condition. In addition, SIMPLE-Consistent (SIMPLEC) algorithm has been utilized for coupling pressure-velocity in the simulation part. Second order upwind scheme has been selected in solving energy and momentum equations. Moreover, convergence criterion for continuity, velocity and also energy were determined as 10^{-5}, 10^{-5} and 10^{-7}, respectively.

Mass conservation equation:

$$\frac{\partial \rho}{\partial t} + \nabla.(\rho\vec{v}) = 0 \tag{1}$$

Momentum conservation equation:

$$\frac{\partial}{\partial t}(\rho\vec{v}) + \nabla.(\rho\vec{v}\vec{v}) = -\nabla p + \nabla.(\bar{\bar{\tau}}) + \rho\vec{g} + \vec{F} \tag{2}$$

here $\bar{\bar{\tau}}$ presents stress tensor, p demonstrates pressure, $\rho\vec{g}$ illustrates gravitational force and $\vec{F}$ expresses and external force.

Energy conservation equation:

$$\underbrace{\frac{\partial}{\partial t}(\rho E)}_{Unsteady} + \underbrace{\nabla.(\vec{v}(\rho E + p))}_{Convection} = \nabla.\left(\underbrace{k_{eff}\nabla \mathrm{T}}_{Conduction} - \underbrace{\sum_j h_j\vec{J_j}}_{Species\ diffusion} + \underbrace{(\bar{\bar{\tau}}_{eff}\vec{v})}_{Viscous\ dissipation}\right) + \underbrace{S_h}_{Enthalpy\ source/Sink} \quad (3)$$

here k_{eff} denotes thermal conductivity, $\vec{J_j}$ shows diffusion flux of j species and S_h demonstrates heat resources. The first three terms on the right side of Eq. (3) demonstrate energy transfer due to conduction, species diffusion and viscous dissipation, respectively.

In Eq. (3) the term E, can be defined as:

$$E = h - \frac{p}{\rho} + \frac{v}{2} \quad (4)$$

here sensible enthalpy (h) can be defined for incompressible flows as:

$$h = \sum_j Y_j h_j + \frac{p}{\rho} \quad (5)$$

where Y_j shows the mass fraction of species j and:

$$h_j = \int_{T_{ref}}^{T} c_{p,j}\, dT \quad (6)$$

The turbulence kinetic energy (k) and dissipation rate (ε) in RNG k-ε model could be acieved as follows [45]:

$$\frac{\partial}{\partial t}(\rho k) + \frac{\partial}{\partial x_i}(\rho k v_i) = \frac{\partial}{\partial x_j}\left[\alpha_k \mu_{eff}\frac{\partial k}{\partial x_j}\right] + G_k + G_b - \rho\varepsilon - Y_M + S_k \quad (7)$$

$$\frac{\partial}{\partial t}(\rho \varepsilon) + \frac{\partial}{\partial x_i}(\rho \varepsilon v_i) = \frac{\partial}{\partial x_j}\left[\alpha_\varepsilon \mu_{eff}\frac{\partial \varepsilon}{\partial x_j}\right] + C_{1\varepsilon}\frac{\varepsilon}{k}(G_k + C_{3\varepsilon}G_b) - C_{2\varepsilon}\rho\frac{\varepsilon^2}{k} - R_\varepsilon + S_\varepsilon \quad (8)$$

hereG_b represents the turbulence kinetic production because of buoyancy effect, G_k shows the production of turbulence kinetic energy that arise from average velocity gradients, Y_M denotes the influence of the fluctuating expansion in compressible turbulence to the whole dissipation rate, α_k and α_ε are the inverse Prandtl numbers for k and ε, S_ε and S_k illustrate source terms, $G_{3\varepsilon}$, $C_{2\varepsilon}$ and $C_{1\varepsilon}$ are constants.

In addition, the turbulent viscosity (μ_t) can be attained by utilizing k and ε as:

$$\mu_t = \rho C_\mu \frac{k^2}{\varepsilon} \tag{9}$$

2.2. Experimental setup

In this study a shell and helically coiled tube HE has been fabricated by considering simulation outcomes. Fig. 6 presents fabrication steps of shell and helically coiled HE. The fabrication of shell and helically coiled HE has been performed regarding the manufacturing techniques [46, 47]. Helically coiled tube has been fabricated using a copper tube with 1 mm thickness. As mentioned in the numerical simulation section, an extra tube in the middle of HE has been utilized to regulate fluid flow and consequently increase heat transfer rate in the HE. Also, the shell and inner tube of HE fabricated using stainless steel. After the fabrication of the HE, it insulated with the aim of decreasing heat loss. In the shell and helically coiled HE, hot fluid flows over the helically coiled and cold fluid flows in the shell side. In addition, the test setup is presented in Fig. 7. The hot water is warmed up by utilizing an electrical resistance available in the hot water tank and is circulated in the system by using a circulation pump in the hot fluid loop. Also, in the test setup some safety precautions like pressure valves and circuit breakers have been used. In the test setup two flow meters in hot and cold loops with accuracy of ±5% have been used to measure flow rates. Also, to obtain the temperature of cold and hot fluids thermocouples with accuracy of 0.5°C have been utilized in the test setup. A dimmer is available in the test system to adjust the intended power for the electrical heater. Moreover, a control system is available in the experimental setup. As it is mentioned, hot fluid warmed up in the hot water tank and distributed to the helically coiled tube of the HE. While, cold fluid flows inside the shell loop of the HE and absorbs heat from hot side and discharged from the setup.

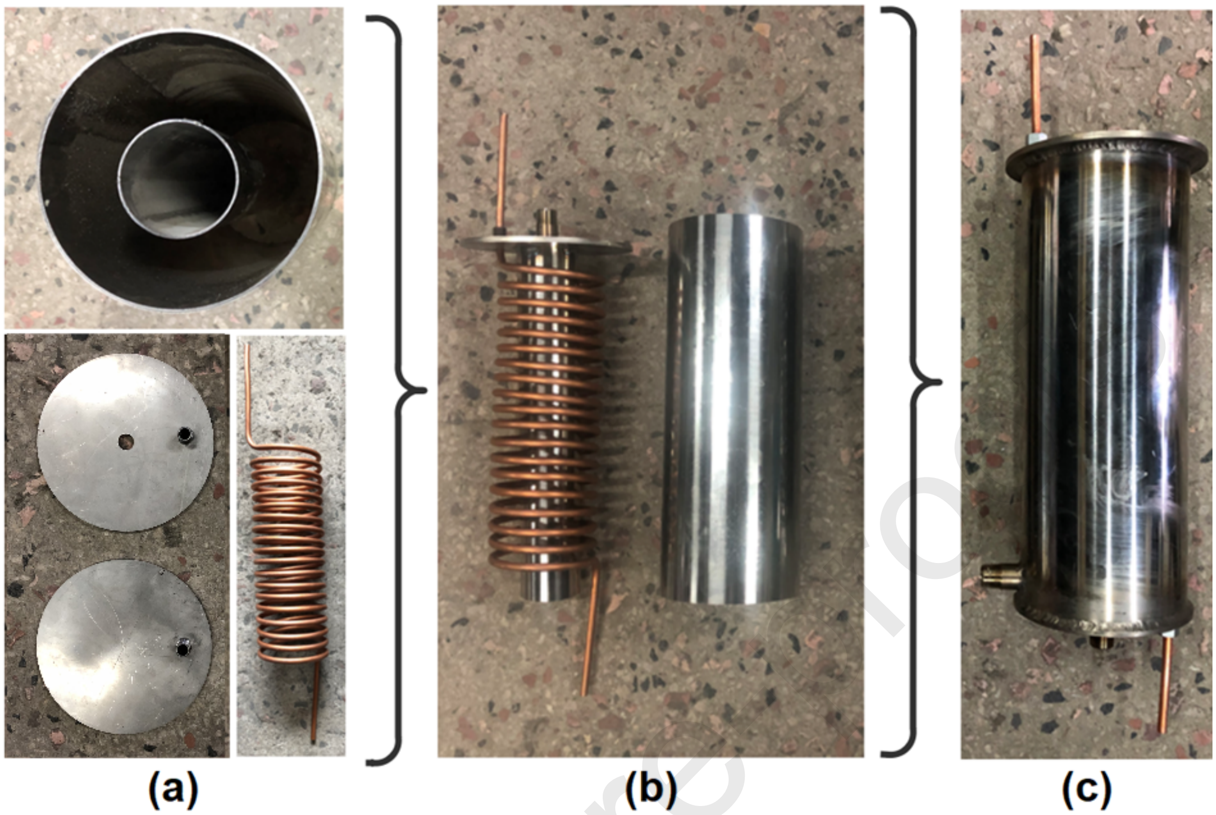

Fig. 6. Fabrication steps of shell and helically coiled HE; (a) components, (b) placement of the helical coil, (c) final assembly

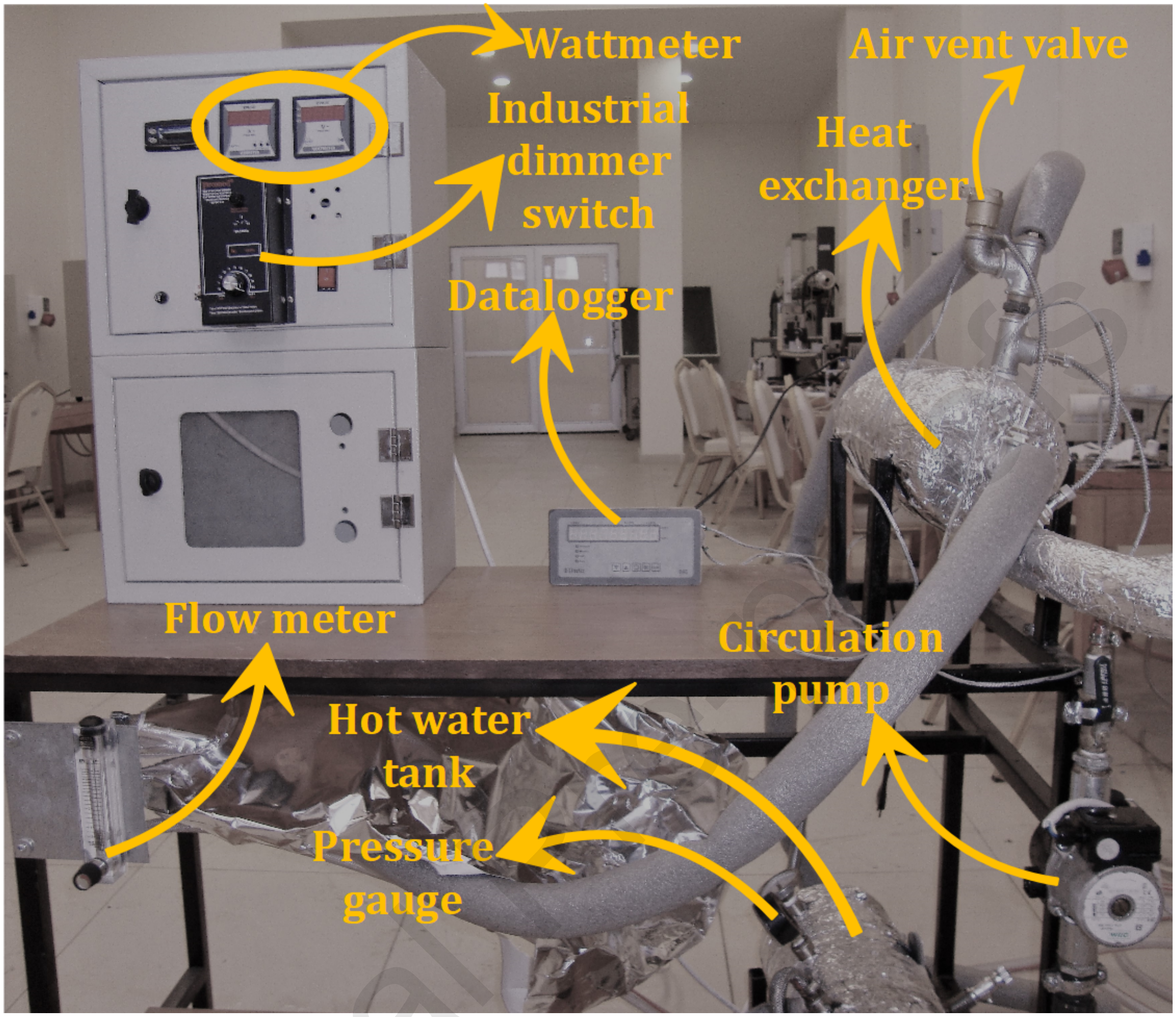

Fig. 7. Experimental setup

2.5. Experimental procedure

The performance tests of shell and helically coiled HE have been conducted to determine heat transfer and flow behavior. The performance tests have been done in 3 different flow rates of cold and hot fluid. In the experiments, the inlet temperature of hot fluid has been adjusted to a set temperature and after reaching steady conditions the values have been recorded. Moreover, to obtain accurate findings all tests have been repeated five times.

2.4. Calculations

In this section utilized equations in analysis of experimental findings are given. Transferred thermal energy in the cold loop ($\dot{Q}_{cold}$) and hot loop ($\dot{Q}_{hot}$) can be obtained by using Eq. (10) and Eq. (11). It is better to state that average values of specific heat capacity were utilized in the calculations.

$$\dot{Q}_{hot} = \dot{m}_{hot}.c_{p,hot}.(T_{hot,\,in} - T_{hot,\,out}) \quad (10)$$

$$\dot{Q}_{cold} = \dot{m}_{cold}.c_{p,cold}.(T_{cold,\,out} - T_{hot,\,in}) \quad (11)$$

Generally, transferred heat in the hot and cold side is not equal to each other because of some factors like heat loss. However, heat transfer in the cold and hot loop can be assumed to be equal to simplify the calculations. Therefore, it can be expressed as:

$$\dot{Q}_{hot} = \dot{Q}_{cold} \quad (12)$$

The most important issue in investigating HE is determining the thermal performance of them. In this regard, the effectiveness of HE can be expressed by utilizing Eq. (13).

$$\varepsilon = \frac{\dot{Q}}{\dot{Q}_{max}} = \frac{c_{hot\,fluid}(T_{hot,in} - T_{hot,out})}{C_{min}\,(T_{hot,in} - T_{cold,in})} = \frac{c_{cold\,fluid}(T_{cold,out} - T_{cold,in})}{C_{min}\,(T_{hot,in} - T_{cold,in})} \quad (13)$$

where C_{hot} and C_{cold} denote hot and cold fluids heat capacity rate and could be defined as:

$$C_{hot} = \dot{m}_{hot}.c_{p,hot} \quad (14)$$

$$C_{cold} = \dot{m}_{cold}.c_{p,cold} \quad (15)$$

Overall heat transfer coefficient (OHTC) in the HE as an important parameter in analyzing thermal performance can be written as follows:

$$U = \frac{\dot{Q}}{A\,(\Delta T_{LMTD})} \quad (16)$$

where A shows the outer surface area of the coil and ΔT_{LMTD} demonstrates the logarithmic mean temperature difference. ΔT_{LMTD} is calculated following equation:

$$\Delta T_{LMTD} = \frac{\Delta T_{in} - \Delta T_{out}}{ln\left(\frac{\Delta T_{in}}{\Delta T_{out}}\right)} \quad (17)$$

The Reynolds number is utilized in determining the flow regime. The Reynolds number in the helical tube side of the HE can be expressed as follows [10]:

$$Re_{coil} = 2100\left[1 + 12(\mathrm{d_{inner}}/\mathrm{D_{coil}})^{1/2}\right] \quad (18)$$

Also, Dean number could be defined as:

$$De = Re_{coil}\left(\frac{d_{inner}}{\mathrm{D_{coil}}}\right)^{0.5} \quad (19)$$

The Nusselt number in coil side could be determined by using Eq. (20) [8].

$$Nu_{coil} = 0.0456\left(\frac{\mathrm{D_{coil}}}{d_{inner}}\right)^{-0.16} Re_c^{0.8} Pr_c^{0.4} \quad (20)$$

The Reynolds number in shell side of the HE could be achieved as follows:

$$Re_{shell} = \frac{\rho V D_{h,shell}}{\mu} \quad (21)$$

The Nusselt in shell side (outside of coil) could be obtained by using Eq. (22) and Eq. (23) [10].

$$\mathrm{Nu_{shell}} = 0.6\ \mathrm{Re_{shell}^{0.5}}\ \mathrm{Pr_{shell}^{0.31}} \quad \text{for } 50 < Re < 10000 \quad (22)$$

$$\mathrm{Nu_{shell}} = 0.224\ \mathrm{Re_{shell}^{0.6}}\ \mathrm{Pr_{shell}^{0.33}} \quad \text{for } 6000 < \mathrm{Re} < 10000 \quad (23)$$

It must be stated that Nusselt number in the shell side and tube side can be obtained by using the related hydraulic diameter of each side:

$$Nu_{coil} = \frac{h_{inner} d_{inner}}{k} \quad (24)$$

$$Nu_{shell} = \frac{h_{shell} D_{h,shell}}{k} \quad (25)$$

where d_{inner} denotes the hydraulic diameter of coil side and $D_{h,shell}$ is the hydraulic diameter of the shell side that could be calculated as:

$$D_{h,shell} = \frac{4\ \times Volume\ of\ shell\ side}{Contact\ surface\ with\ fluid} \quad (26)$$

The uncertainties of experimental investigations can be derived from measurement devices type, device calibration, experimental conditions, and connection points [48]. The overall experimental uncertainty could be achieved by utilizing Eq. (27) [49, 50].

$$\mathrm{W_R} = \left[\left(\frac{\partial R}{\partial x_1} w_1\right)^2 + \left(\frac{\partial R}{\partial x_2} w_2\right)^2 + \dots + \left(\frac{\partial R}{\partial x_n} w_n\right)^2\right]^{1/2} \quad (27)$$

Uncertainty values were given in Table 3. Khanlari et al. [51] found uncertainty value for flow rate as ±5.36%. Panahi and Zamzamian [52] obtained uncertainty values for HTC and effectiveness as ±9.17% and ±10.2%, respectively. Elshazly et al. [53] achieved experimental uncertainty value of HTC in the range of 4.7-7.0%. As it can be seen, obtained experimental uncertainty values of this study are in good agreement with the literature.

Table 3. Experimental uncertainty values

Parameter	Unit	Uncertainty
Temperature	°C	±0.58
Flow rate	%	±5.12
Heat transfer coefficient	%	±6.64
Effectiveness	%	±7.48

3. Results and discussion

In this section experimentally and numerically obtained results of analyzing shell and helically coiled HE are given and explained in detail.

3.1. Numerical simulation results

As mentioned above in this study a modified shell and helically coiled HE has been analyzed and compared with a conventional one. Fig. 8 presents temperature distribution in the helically coiled tube for conventional and modified HEs. As can be seen in Fig. 8, the temperature distribution in modified HE is more homogeneous in comparison with the conventional one. In other words, the temperature over the different zones of the coiled tube in the modified HE is similar. The main reason for this fact is using an extra tube inside the shell side of HE. Fig. 9 demonstrates the temperature distribution in the shell side from side view for conventional and modified heat exchangers. Fig. 9 presents how cold water enters the heat exchanger, warms up and leaves the heat exchanger. As can be clearly seen in Fig. 9, cold water in the modified heat exchanger gained more energy in comparison with the conventional one. The main reason for gaining more energy by cold water in modified heat exchanger is regulating flow distribution by using a new design. Velocity distribution in the shell side of shell and helically coiled HEs from the side view is demonstrated in Fig. 10. As stated above the first heat exchanger positioned in the vertical state and the second heat exchanger positioned in the horizontal state. The velocity of water in the regions near the helically coiled tube in the shell side of the modified HE is relatively low in comparison with other regions that is the main reason for the increasing heat exchange rate in the modified HE. As can be clearly seen in Fig. 10, cold fluid enters to the HE along a hollow tube integrated to the shell side. Utilizing this additional hollow tube led to obtaining more homogeneous flow distribution in comparison with the conventional type. This fact caused to improve heat exchange rate in the modified type HE. Utilizing this modification regulated the fluid flow in the shell side and improved the thermal efficiency of HE. In other words, this modification leads to a change in water flow pattern in the shell side of the heat exchanger and increases the heat exchange rate. Fig. 11 illustrates cold side outlet temperature variation with flow rate for conventional and modified heat exchangers. Fig. 11 shows successful utilization of new configuration for shell and helically coiled heat exchanger. Outlet temperature of cold water in modified heat exchanger averagely improved as 10% in comparison with conventional one. Simulation results indicates the effective design of the modified shell and helically coiled HE. Therefore, fabricated HE in this study developed by considering numerical simulation results.

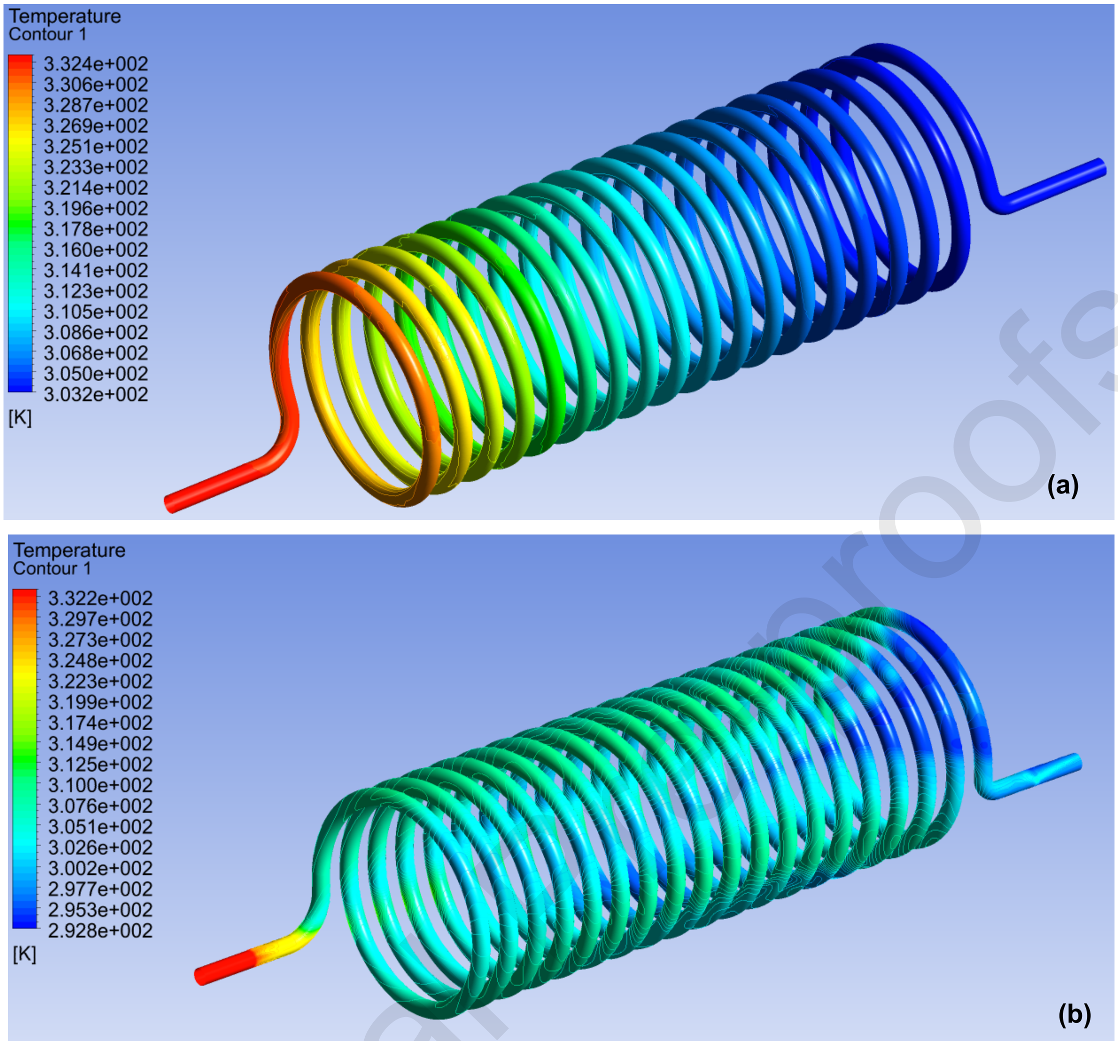

Fig. 8. Temperature distribution in helicaaly coiled tube; a) Conventional type; b) Modified type

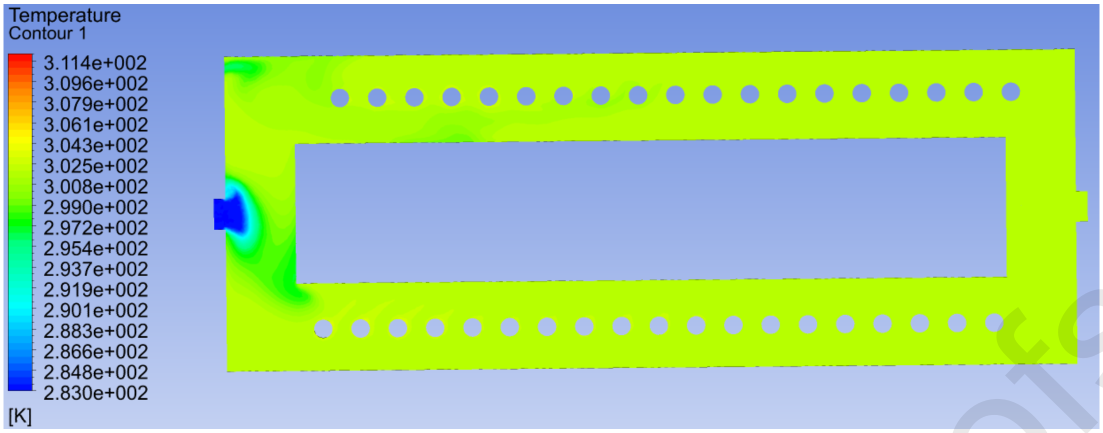

(a)

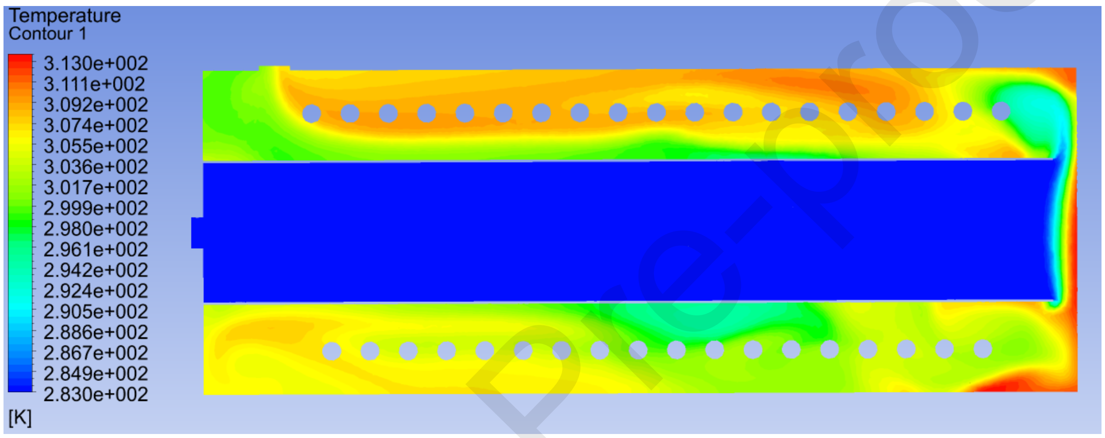

(b)

Fig. 9. Temperature distribution in shell side from side view; a) Conventional type; b) Modified type

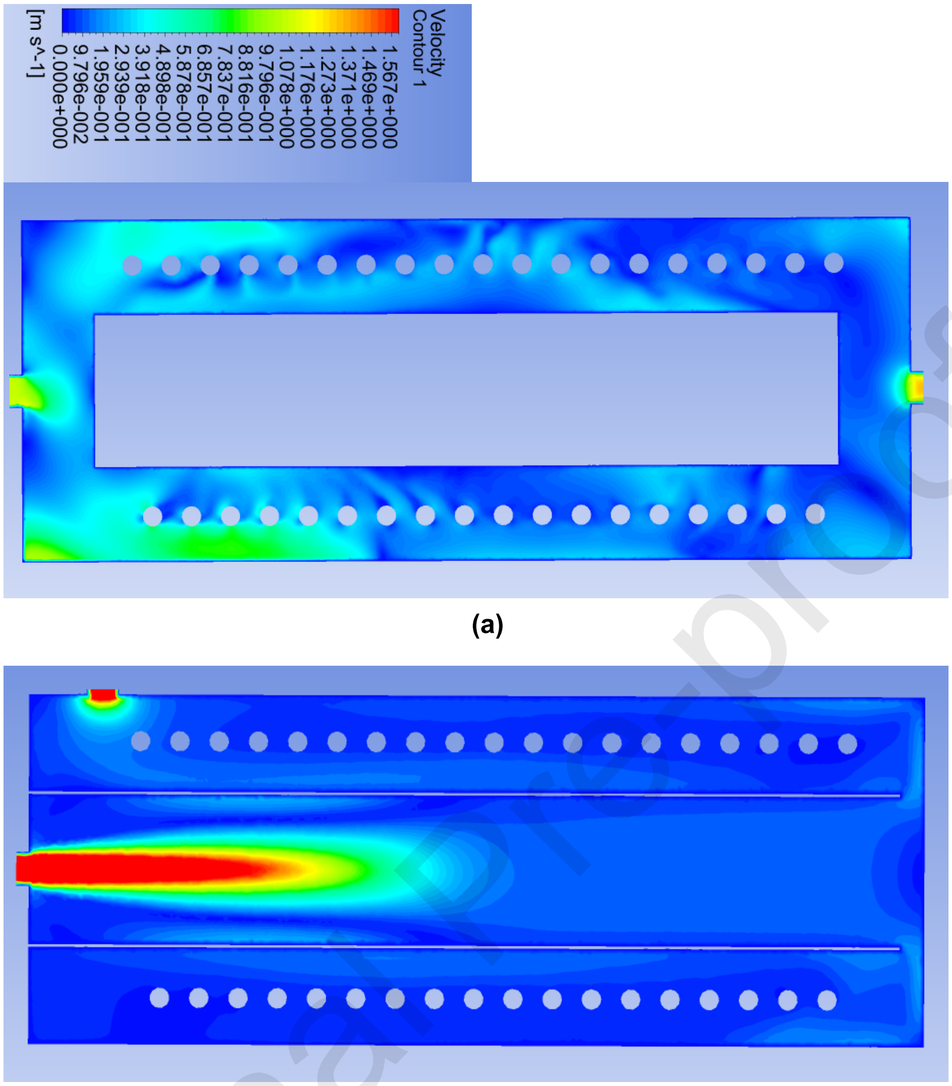

Fig. 10. Velocity distribution in shell side from side view; a) Conventional type; b) Modified type

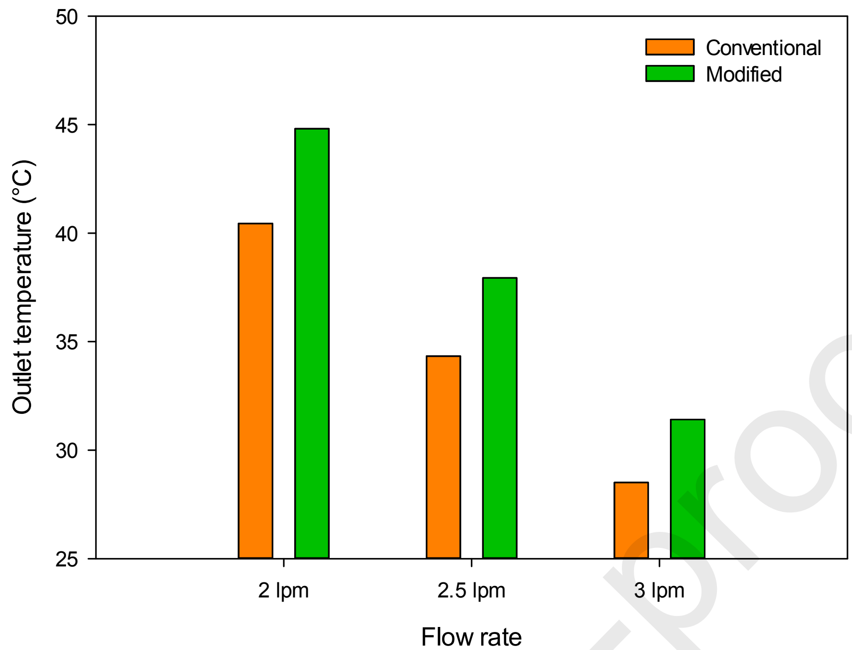

Fig. 11. Cold side outlet temperature variation with flow rate

3.2. Experimental results

Fig. 12. presents average transferred heat in the HE with respect to hot side inlet temperature. As it is seen in Fig. 12 transferred heat increases with raising inlet temperature in the HE for all Reynolds numbers. Also, it is seen that increasing Reynolds number led to increase in the transferred heat. Increasing the Reynolds number led to a maximum improvement of 42% in heat transfer rate. In addition, transferred heat in cold and hot side of the HE with respect to hot side inlet temperature is demonstrated in Fig. 13. As it is obviously seen in Fig. 13, released heat in the hot side and absorbed heat in the cold side are so close to each other. This fact indicates low experimental errors that arose from good heat insulation utilized in the HE. The maximum difference between released heat in the hot side and absorbed heat in the cold side is 5%. The obtained heat transfer rate in this study varied between 2000-4600 W. In a study done by Bahrehmand and Abbassi [54] the rate of heat transfer was obtained in the range of 3500-14000 Win a shell and helically coiled HE. In another study, Srinivas and Venu Vinod [55] achieved heat transfer rate between 800-6000 W in a similar helically coiled HE. Alimoradi et al.

[56] investigated a shell and helically coiled finned HE in the Reynolds number between 7500-30000 and obtained the rate of heat transfer in the range of 3800-8000 W. Also, Barzegari et al. [57] attained the rate of heat transfer in the range of 2200-9500 in a helically coiled HE. It is better to state that geometrical parameters in the given works are not the same. However, the obtained heat transfer values in the present research are in good accordance with similar works.

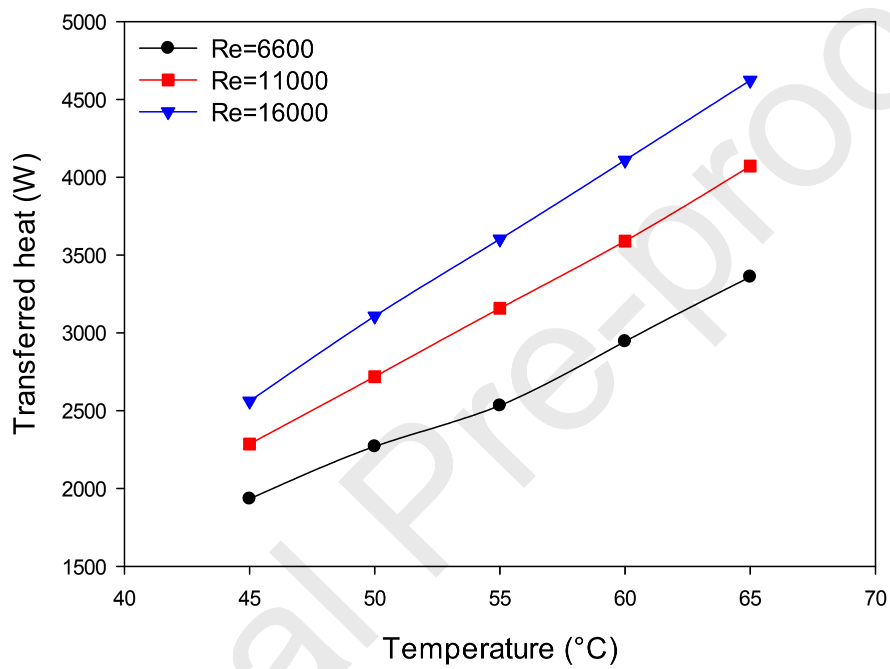

Fig. 12. Average transferred heat in the HE with respect to hot side inlet temperature

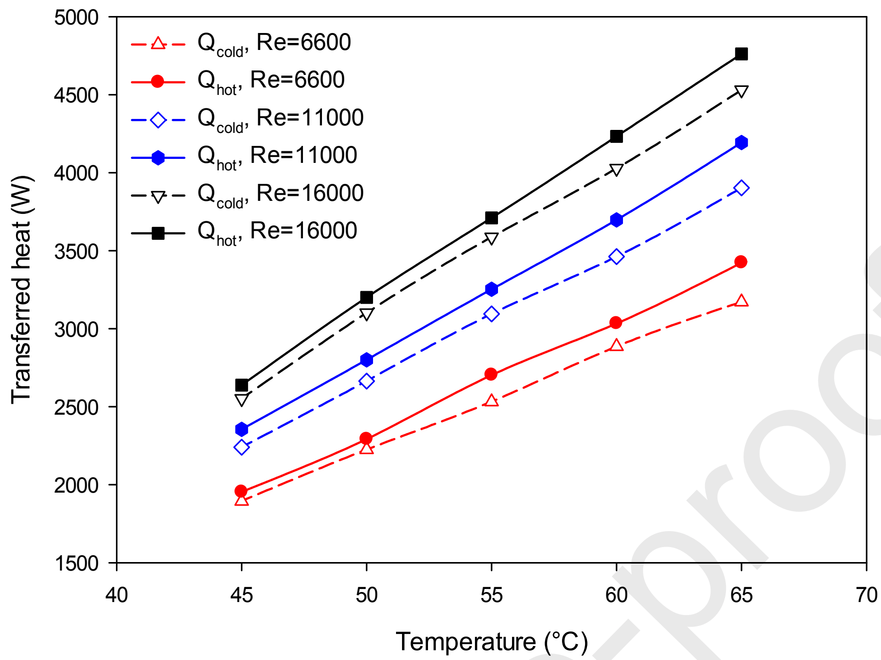

Fig. 13. Transferred heat in cold and hot side of the HE with respect to hot side inlet temperature

Fig. 14 represents the variation of OHTC with respect to hot side inlet temperature. Fig. 14 shows that raising Reynolds number led to increase in the OHTC. Increasing Reynolds number from 6600 to 16000 led to a maximum increment of 40% in OHTC. In this study, OHTC obtained in the range of 1600-3150 W/m^{2}K. In a study performed by Bahrehmand and Abbassi [54] OHTC obtained between 1000-1550 W/m^{2}K in a similar HE. Kumar Naik and Vinod [58] obtained OHTC in a helically coiled HE in the range of 500-3500 W/m^{2}K by using water and nanofluid. Salem et al. [59] tested a shell and helically coiled HE and obtained OHTC between 200-1500 W/m^{2}K. Panahi and Zamzamian [52] obtained OHTC between 400-1700 W/m^{2}K in a shell and helically coiled HE with helical wire modification. In addition, Niwalkar et al. [60] attained OHTC in the range of 800-2800 W/m^{2}K in a shell and helically coiled HE.

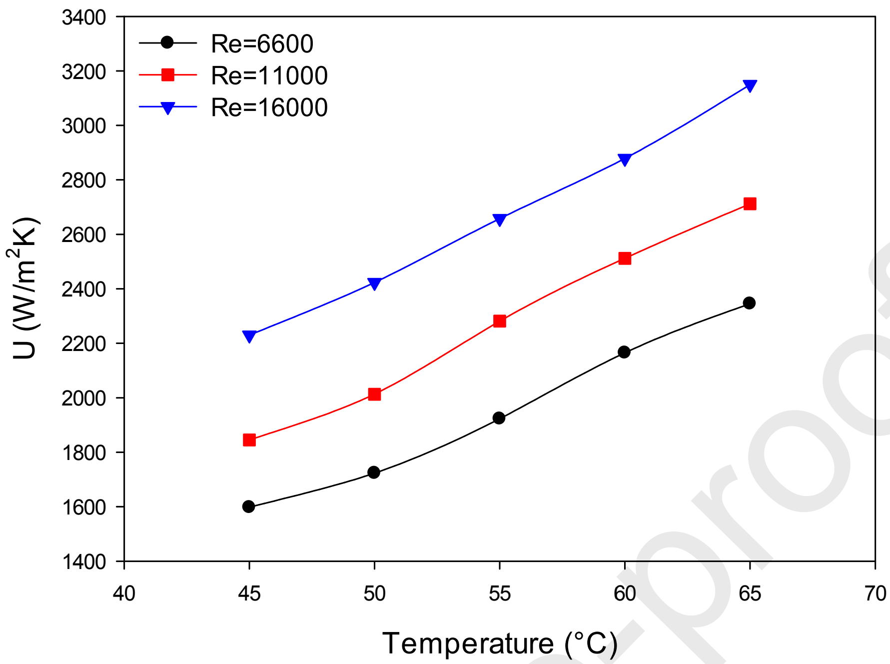

Fig. 14. Variation of OHTC with respect to hot side inlet temperature

Fig. 15 represents the change in HTC of coil side with respect to hot side inlet temperatures. As it can be seen in Fig. 15, Reynolds number has a significant effect on the HTC. Increasing Reynolds number leads to increase in turbulence intensity which improves the HTC in the HE. In addition, HTC increased by increasing the temperature. HTC of coil side in this study was obtained in the range of 5700-13400 W/m^{2}K. Niwalkar et al. [60] attained HTC in the range of 2000-14000 W/m^{2}K in a shell and helically coiled HE by utilizing water and nanofluid as working fluid. Palanisamy and Mukesh Kumar [61] attained HTC between 3800-6800 W/m^{2}K in a shell and cone helically coiled HE. Fule et al. [62] achieved HTC in coil side of a shell and helically coiled HE up to 7000 W/m^{2}K. Also, Bahrehmand and Abbassi [54] obtained HTC in coil side of a shell and helically coiled HE as 5000-25000 W/m^{2}K.

Variation of HTC of shell side with respect to Reynold number and at different cold side outlet temperatures is given in Fig. 16. As it is seen, increasing the Reynolds number and the temperature caused to improve in HTC of shell side. In this work, HTC of shell side was obtained between 2250-4050 W/m^{2}K. In a study, Bahrehmand and Abbassi [54] obtained HTC in shell side as 1100-1500 W/m^{2}K.

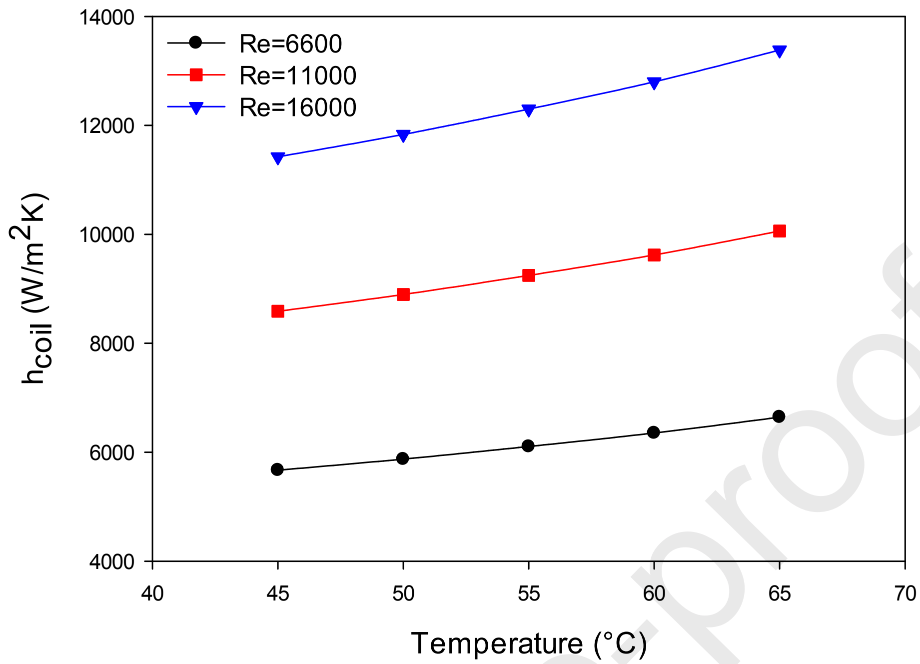

Fig. 15. Variation of HTC of coil side with respect to hot side inlet temperature

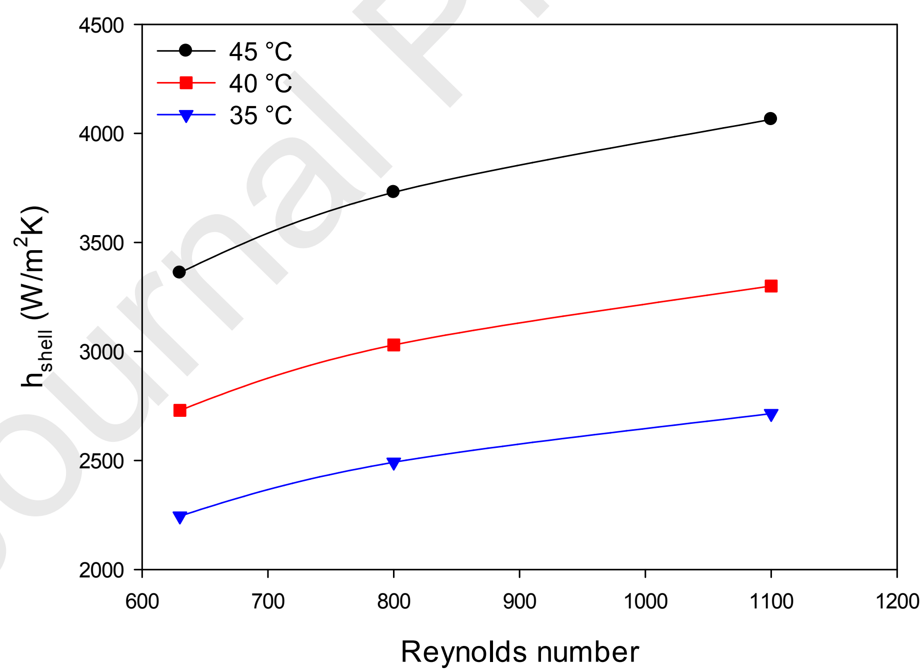

Fig. 16. Variation of HTC of shell side with respect to Reynold number

Fig. 17 shows variation of Nusselt number of coil side via hot side inlet temperature. Higher Reynolds number led to obtain higher Nusselt number as can be seen in Fig 17. Also, by increasing hot side inlet temperature, Nusselt number are also increased slightly. In this study, Nusselt number in coil side was obtained in the range of 53-125. In a study performed by Andrzejczyk and Muszynski [63] Nusselt number in coil side obtained between 20-130. Etghani and Hosseini Baboli [27] achieved Nusselt number in coil side of HE in the range of 53-76. Kannadasan et al. [13] achieved Nusselt number in the range of 35-105 in a helically coiled HE. Jamshidi et al. [7] attained the Nusselt number between 40-80 in a shell and helically coiled HE. Wang et al. [64] investigated a shell and helically coiled finned HE and average Nusselt obtained as 110. Alimoradi and Veysi [65] achieved the Nusselt number between 35-165 in a horizontal shell and helically coiled HE. Wang et al. [29] attained the Nusselt number in the range of 25-375 in a shell and helically twisted-coiled HE. Sepehr et al. [66] analyzed a shell and helically coiled finned tube HE and achieved average Nusselt number about 125. They indicated that using finned tube has significant positive effect on heat transfer. As it is seen, obtained Nusselt number in this research is in acceptable range in comparison with related studies in the literature.

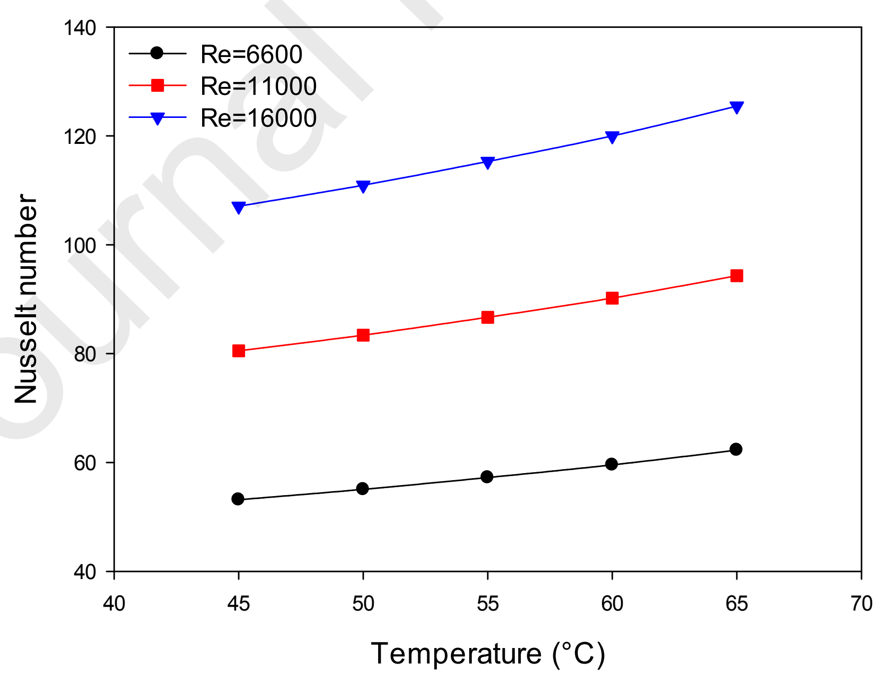

Fig. 17. Variation of Nusselt number of coil side via hot side inlet temperature

Fig. 18 presents effectiveness variation via temperature in the HE. Increasing the Reynolds number and temperature led to improve in the effectiveness as can be seen in Fig. 18. The effectiveness in the present research was obtained in the range of 0.59-0.87 for different working conditions. In a study Baqir et al. [67] obtained the effectiveness in the range of 0.50-84 in a shell and helically coiled HE with air injection. Srinivas and Venu Vinod [55] tested a shell and helically coiled HE and obtained the effectiveness in the range of 0.60-1. Bahrehmand and Abbassi [54] achieved effectiveness in the range of 0.39-0.54 in a similar HE. Alimoradi [68] experimentally and numerically analyzed a shell and helically coiled HE and achieved the effectiveness in the range of 0.25-0.85.

Fig. 19 illustrates a comparison between numerically and experimentally obtained outlet temperatures of cold side. As it is seen in Fig. 19, there is a good accordance among numerical and experimental outlet temperature. It is better to state that the numerical results in Fig. 19 were obtained using RNG k-ε model. The average deviation between numerical and experimental outlet temperature is 8%. As mentioned above, different models have been tested in the numerical analysis part of this study and finally RNG k-ε model has been selected to be utilized. Fig. 20 presents shell side outlet temperature for different turbulence models. As it can be seen in Fig. 20, RNG k-ε model gave the closest result to the experimental data.

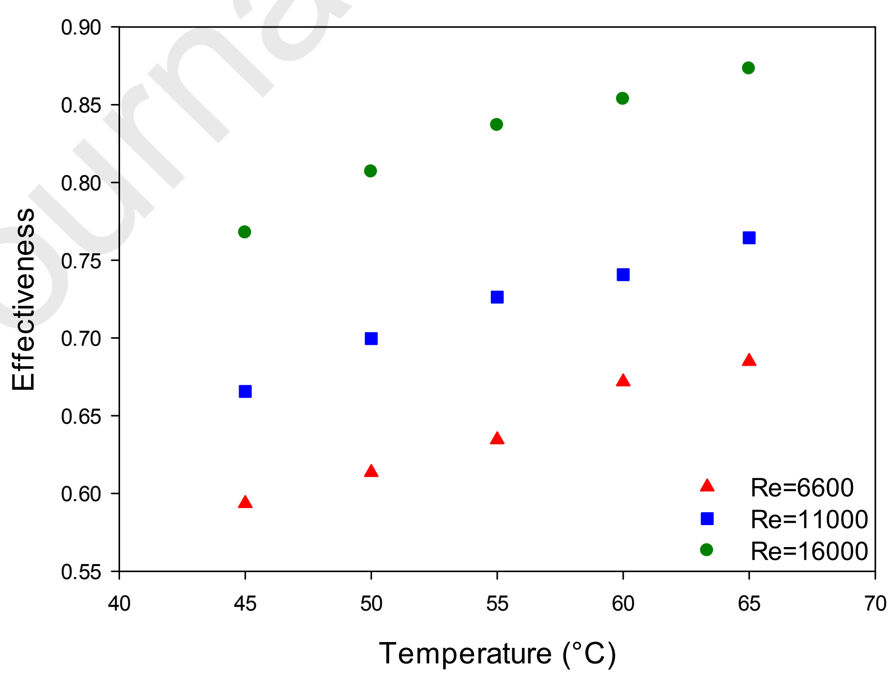

Fig. 18. Effectiveness variation via temperature

A general comparison between the results of this work and similar studies in the literature are presented in Table 4. Different parameters such as flow rate, HTC, OHTC, Reynolds number and Nusselt number are given for various studies. Comparing the obtained results of this study with other studies shows an acceptable agreement between them. In addition, it is useful to state that the size of HEs presented in Table 3 are not same. This fact makes it difficult to perform a sensitive comparison between the presented studies. Numerical and experimental outcomes of this study indicated the successful design of shell and helically coiled HE. The suggested modification for shell and helically coiled HE led to improve the HE's thermal performance. The main reason for this improvement is obtaining regular and homogeneous flow in the shell side of the HE that is a result of adding a hollow tube into the shell side.

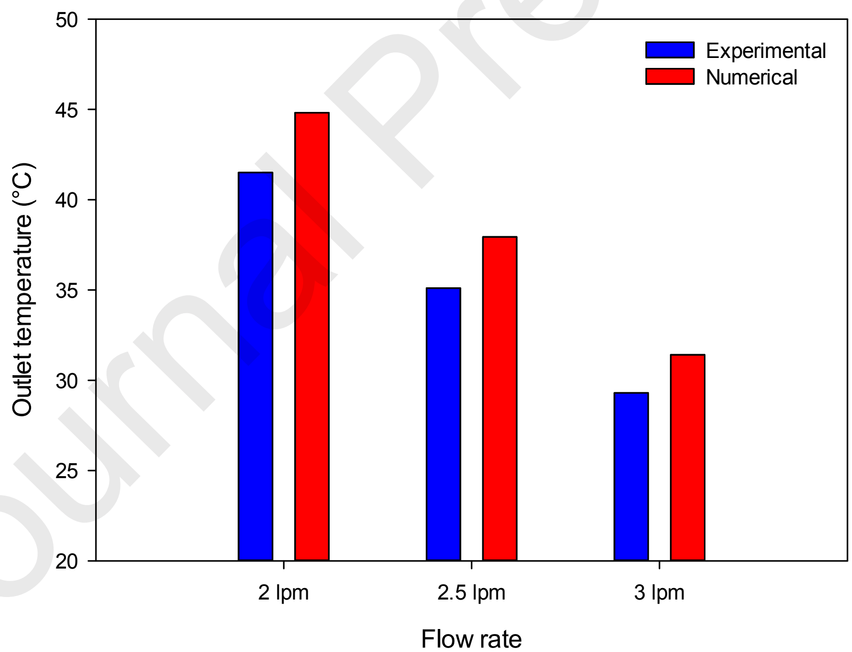

Fig. 19. Comparison between numerical and experimental outlet temperature

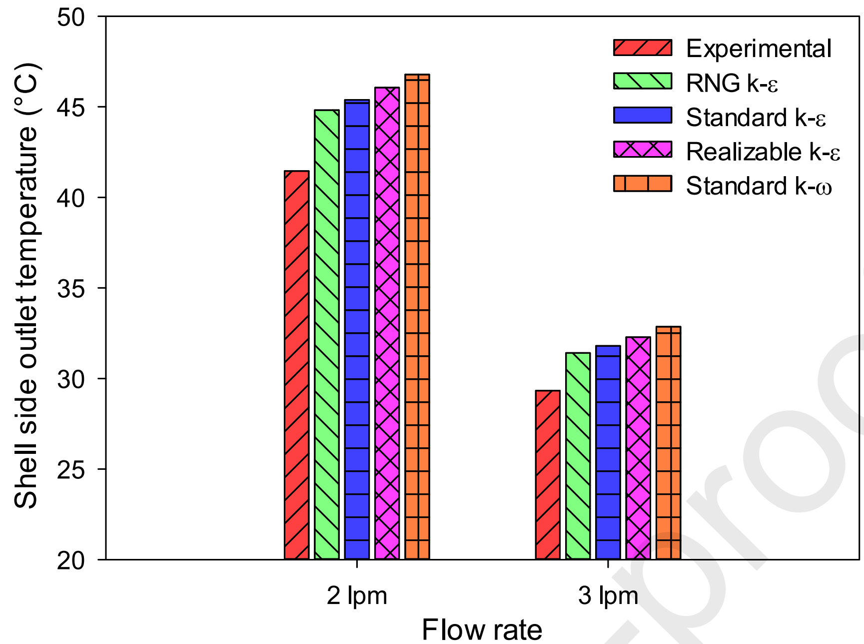

Fig. 20. Shell side outlet temperature for different turbulence models

Table 4. A general comparison between this work and similar studies in the literature

Ref.	Application		Flow rate	Coil side Reynolds number	$\dot{Q}$ (W)	h_{coil} (W/m²K)	h_{Shell} (W/m²K)	U (W/m²K)	Nu_{coil}
	Exp	Num							
Barzegari et al. [57]	✓	-	2-3.5 lpm	10800-21182	2200-9500	2150-3000	-	-	16-20
Zaboli et al. [69]	-	✓	1-4 lpm	1300-5270	-	500-3000	-	-	40-85
Elshazly et al. [53]	✓		1.7-11.15 lpm	5700-55000	-	2000-2700	-	500-2000	20-270
Jamshidi et al. [7]	✓	-	1-4 lpm	2000-1000	-	-	-	625-1100	40-80
Panahi, and Zamzamian [52]	✓	-	1-5 lpm	4000-18000	-	-	-	400-1700	-
Salem et al. [59]	✓	-	1.7-11 lpm	10000-60000	-	-	-	200-1500	50-240
Niwalkar et al. [60]	✓	-	0.5-0.84 lpm	1500-4200	-	2000-14000	-	800-2800	15-130
Bahrehmand and Abbassi [54]	-	✓	0.3-0.113 kg/s	10000-35000	3500-14000	5000-25000	1100-1500	1000-1550	40-140
This study	✓	✓	1.5-3.5 lpm	6600-16000	2000-4600	5700-13400	2250-4050	1600-3150	53-125

4. Conclusion

In this study, thermal performance of a shell and helically coiled HE has been improved by utilizing a new modification. In the first step of the study, the performance of modified shell and helically coiled HE has been compared with a conventional vertical shell and helically coiled HE by using CFD approach to determine appropriate configuration. In the second step of the study, the modified HE has been manufactured considering CFD simulation results. The fabricated modified HE has been experimentally tested at various conditions to determine its effectiveness. Numerical and experimental findings of this study showed the successful design of the modified HE. The suggested simple modification for shell and helically coiled HE led to improve the HE's thermal performance. The main reason for improvement of HE's thermal performance is obtaining regular and homogeneous flow over the coiled tube in the shell side of the HE that is a result of adding a hollow tube into the shell side. Experimental results indicated that increasing Reynolds number and hot fluid's inlet temperature led to improve in the OHTC. The effectiveness of modified shell and helically coiled HE was obtained in the range of 0.59-0.87 at different working conditions. Also, the average deviation between numerical and experimental outlet temperature is 8%.

References

[1] Z. Lu, L. Wang, R. Wang, Experimental analysis of an adsorption refrigerator with mass and heat-pipe heat recovery process, Energy Conversion and Management 53 (2012) 291-297.

[2] M. Omidi, M. Farhadi, M. Jafari, A comprehensive review on double pipe heat exchangers, Applied Thermal Engineering 110 (2017) 1075-1090.

[3] J.D. Moya-Rico, A.E. Molina, J.F. Belmonte, J.I. Córcoles Tendero, J.A. Almendros-Ibáñez, Experimental characterization of a double tube heat exchanger with inserted twisted tape elements, Applied Thermal Engineering 174 (2020) 115234.

[4] Y. Lv, K. Lu, Y. Ren, Composite crystallization fouling characteristics of normal solubility salt in double-pipe heat exchanger, International Journal of Heat and Mass Transfer 156 (2020) 119883.

[5] A.K. Satapathy, Thermodynamic optimization of a coiled tube heat exchanger under constant wall heat flux condition, Energy 34 (2009) 1122-1126.

[6] Colorado D, Ali ME, García-Valladares O, Hernández JA. Heat transfer using a correlation by neural network for natural convection from vertical helical coil in oil and glycerol/water solution, Energy 36 (2011) 854-863.

[7] N. Jamshidi, M. Farhadi, D.D. Ganji, K. Sedighi, Experimental analysis of heat transfer enhancement in shell and helical tube heat exchangers, Applied Thermal Engineering 51 (2013) 644-652.

[8] B.K. Hardik, P.K. Baburajan, S.V. Prabhu, Local heat transfer coefficient in helical coils with single phase flow, International Journal of Heat Mass Transfer 89 (2015) 522-538.

[9] H. Sadighi Dizaji, S. Jafarmadar, M. Hashemian, The effect of flow, thermodynamic and geometrical characteristics on exergy loss in shell and coiled tube heat exchangers, Energy 91 (2015) 678-684.

[10] R. Ramesh, S.N. Murugesan, C. Narendran, R. Saravanan, Experimental investigations on shell and helical coil solution heat exchanger in NH_3-H_2O vapour absorption refrigeration system (VAR), International Communications in Heat and Mass Transfer 87 (2017) 6-13.

[11] R. Andrzejczyk, T. Muszynski, An experimental investigation on the effect of new continuous core-baffle geometry on the mixed convection heat transfer in shell and coil heat exchanger, Applied Thermal Engineering 136 (2018) 237-251.

[12] S. Khorasani, A. Moosavi, A. Dadvand, M. Hashemian, A comprehensive second law analysis of coil side air injection in the shell and coiled tube heat exchanger: An experimental study, Applied Thermal Engineering 150 (2019) 80-87.

[13] N. Kannadasan, K. Ramanathan, S. Suresh, Comparison of heat transfer and pressure drop in horizontal and vertical helically coiled heat exchanger with CuO/water based nano fluids, Experimental Thermal and Fluid Science 42 (2012) 64-70.

[14] R. Andrzejczyk, T. Muszynski, M. Gosz, Experimental investigations on heat transfer enhancement in shell coil heat exchanger with variable baffles geometry, Chemical Engineering & Processing: Process Intensification 132 (2018) 114-126.

[15] S. Khorasani, A. Dadvand, Effect of air bubble injection on the performance of a horizontal helical shell and coiled tube heat exchanger: An experimental study, Applied Thermal Engineering 111 (2017) 676-683.

[16] M. Miansari, M. A. Valipour, H. Arasteh, D.Toghraie, Energy and exergy analysis and optimization of helically grooved shell and tube heat exchangers by using Taguchi experimental design, Journal of Thermal Analysis and Calorimetry 139 (2020) 3151-3164.

[17] A.K. Solanki, R. Kumar, Condensation of R-134a inside dimpled helically coiled tube-in-shell type heat exchanger, Applied Thermal Engineering 129 (2018) 535-548.

[18] M. Rahimi, M.J. Hosseini, M. Gorzin, Effect of helical diameter on the performance of shell and helical tube heat exchanger: An experimental approach, Sustainable Cities and Society 44 (2019) 691-701.

[19] A. Alimoradi, F. Veysi, Optimal and critical values of geometrical parameters of shell and helically coiled tube heat exchangers, Case Studies in Thermal Engineering (2017) 73-78.

[20] F. Afshari, H.G. Zavaragh, G. Di Nicola, Numerical analysis of ball-type turbulators in tube heat exchangers with computational fluid dynamic simulations, International Journal of Environmental Science and Technology 16 (2019) 3771-3780.

[21] N.H. Abu-Hamdeh, R.A.R. Bantan, I. Tlili, Analysis of the thermal and hydraulic performance of the sector-by-sector helically coiled tube heat exchangers as a new type of heat exchangers, International Journal of Thermal Sciences 150 (2020) 106229.

[22] C.K. Mangrulkar, A.S. Dhoble, S. Chamoli, A. Gupta, V.B. Gawande, Numerical optimization of design parameters for a modified double-layer microchannel heat sink, International Journal of Heat and Mass Transfer 138 (2019) 373-389.

[23] C. Yang, P.K. Bansal, Numerical investigation of capillary tube-suction line heat exchanger performance, Applied Thermal Engineering 25 (2005) 2014-2028.

[24] H. Mirgolbabaei, Numerical investigation of vertical helically coiled tube heat exchangers thermal performance, Applied Thermal Engineering 136 (2018) 252-259.

[25] Z. Cancan, W. Dingbiao, X. Sa, H. Yong, P. Xu, Numerical investigation of heat transfer and pressure drop in helically coiled tube with spherical corrugation, International Journal of Heat and Mass Transfer 113 (2017) 332-341.

[26] M. Omidi, M. Farhadi, A.A. Rabienataj Darzi, Numerical study of heat transfer on using lobed cross sections in helical coil heat exchangers: Effect of physical and geometrical parameters, Energy Conversion and Management 176 (2018) 236-245.

[27] M.M. Etghani, SA. Hosseini Baboli, Numerical investigation and optimization of heat transfer and exergy loss in shell and helical tube heat exchanger, Applied Thermal Engineering 121 (2017) 294-301.

[28] H. Chen, Q. L., Y. Liua, B. Gao, Optimal design of a novel non-isometric helically coiled recuperator for Joule–Thomson cryocoolers, Applied Thermal Engineering 167 (2020) 114763.

[29] G. Wang, T. Dbouk, D. Wang, Y. Pei, X. Peng, H. Yuan, S. Xiang, Experimental and numerical investigation on hydraulic and thermal performance in the tube-side of helically coiled-twisted trilobal tube heat exchanger, International Journal of Thermal Sciences 153 (2020) 106328.

[30] Z. Wu, F. Yang, L. Zhu, P. Feng, Z. Zhang, Y. Wang, Improvement in hydrogen desorption performances of magnesium based metal hydride reactor by incorporating helical coil heat exchanger, International Journal Of Hydrogen Energy 41 (2016) 16108-16121.

[31] C.K. Mangrulkar, A.S. Dhoble, P.K. Pant, N. Kumar, A. Gupta, S. Chamoli, Thermal performance escalation of cross flow heat exchanger using in-line elliptical tubes, Experimental Heat Transfer (2019), DOI:10.1080/08916152.2019.1704946.

[32] G. Wang, D. Wang, X. Peng, L. Han, S. Xiang, F. Ma, Experimental and numerical study on heat transfer and flow characteristics in the shell side of helically coiled trilobal tube heat exchanger, Applied Thermal Engineering 149 (2019) 772-787.

[33] G. Wang, D. Wang, J. Deng, Y. Lyu, Y. Pei, S. Xiang, Experimental and numerical study on the heat transfer and flow characteristics in shell side of helically coiled tube heat exchanger based on multi-objective optimization, International Journal of Heat and Mass Transfer 137 (2019) 349-364.

[34] C.K. Mangrulkar, A.S. Dhoble, S. Chamoli, A. Gupta, V.B. Gawande, Recent advancement in heat transfer and fluid flow characteristics in cross flow heat exchangers, Renewable and Sustainable Energy Reviews 113 (2019) 109220.

[35] H.M. Getu, P.K. Bansal, New frost property correlations for aflat-finned-tube heat exchanger, International Journal of Thermal Sciences, 50 (2011) 544-557.

[36] A. Kumar, S. Singh, S. Chamoli, M. Kumar, Experimental investigation on thermo-hydraulic performance of heat exchanger tube with solid and perforated circular disk along with twisted tape insert, Heat Transfer Engineering, 40 (2019) 616-626.

[37] A. Choudhary, M. Kumar, A.K. Patil, S. Chamoli, Enhanced thermal and fluid flow performance of cross flow tube bank with perforated splitter plate, Experimental Heat Transfer (2020) DOI: 10.1080/08916152.2020.1749190.

[38] S. Bhattacharyya, A.C. Benim, M. Pathak, S. Chamoli, A. Gupta, Thermohydraulic characteristics of inline and staggered angular cut baffle inserts in the turbulent flow regime, Journal of Thermal Analysis and Calorimetry 140 (2020) 1519-1536.

[39] A. Kasaeian, S. Babaei, M. Jahanpanah, S. Hamid, A.S. Alsagri, S. Ghaffarian, W.M. Yan, Solar humidification-dehumidification desalination systems: a critical review, Energy Conversion and Management 201 (2019) 112129.

[40] M.R. Salimpour, Heat transfer coefficients of shell and coiled tube heat exchangers, Experimental Thermal and Fluid Science 33 (2009) 203-207.

[41] J.S. Jayakumar, S.M. Mahajani, J.C. Mandal, K.N. Iyer, PK. Vijayan, CFD analysis of single-phase flows inside helically coiled tubes, Computers & Chemical Engineering 34 (2010) 430-446.

[42] S.S. Pawar, V.K. Sunnapwar, Experimental studies on heat transfer to Newtonian and non-Newtonian fluids in helical coils with laminar and turbulent flow, Experimental Thermal and Fluid Science 44 (2013) 792-804.

[43] S. Karagoz, F. Afshari, O. Yildirim, O. Comakli, Experimental and numerical investigation of the cylindrical blade tube inserts effect on the heat transfer enhancement in the horizontal pipe exchangers, Heat and Mass Transfer 53 (2017) 2769-2784.

[44] F. Afshari, H.G. Zavaragh, B. Sahin, R.C. Grifoni, F. Corvaro, B. Marchetti, F. Polonara, On numerical methods; optimization of CFD solution to evaluate fluid flow

around a sample object at low Re numbers, Mathematics and Computers in Simulation 152 (2018) 51-68.

[45] Ansys. ANSYS Fluent Theory Guide. Canonsburg: ANSYS Inc; 2017.

[46] A. Şahinoğlu, M. Rafighi, Investigation of vibration, sound intensity, machine current and surface roughness values of AISI 4140 during machining on the lathe, Arabian Journal for Science and Engineering 45 (2020) 765-778.

[47] A. Şahinoğlu, M. Rafighi, Optimization of cutting parameters with respect to roughness for machining of hardened AISI 1040 steel, Materials Testing 62 (2020) 85-95.

[48] M. Karagöz, Ü. Ağbulut, S. Sarıdemir, Waste to energy: Production of waste tire pyrolysis oil and comprehensive analysis of its usability in diesel engines, Fuel 275 (2020) 117844.

[49] Ü. Ağbulut, M. Karagöz, S. Sarıdemir A. Öztürk, Impact of various metal-oxide based nanoparticles and biodiesel blends on the combustion, performance, emission, vibration and noise characteristics of a CI engine, Fuel 270 (2020) 117521.

[50] Ü. Ağbulut, M. Ayyıldız, S. Sarıdemir, Prediction of performance, combustion and emission characteristics for a dual fuel diesel engine at varying injection pressures, Energy 197 (2020) 117257.

[51] A. Khanlari, D. Yılmaz Aydın, A. Sözen, M. Gürü, H.İ. Variyenli, Investigation of the influences of kaolin-deionized water nanofluid on the thermal behavior of concentric type heat exchanger, Heat Mass Transfer 56 (2020) 1453-1462.

[52] D. Panahi, K. Zamzamian, Heat transfer enhancement of shell-and-coiled tube heat exchanger utilizing helical wire turbulator, Applied Thermal Engineering 115 (2017) 607-615.

[53] K.M. Elshazly, R.Y. Sakr, R.K. Ali, M.R. Salem, Effect of γ-Al_2O_3/water nanofuid on the thermal performance of shell and coil heat exchanger with different coil torsions, Heat Mass Transfer 53 (2017) 1893-1903.

[54] S. Bahrehmand, A. Abbassi, Heat transfer and performance analysis of nanofluid flow in helically coiled tube heat exchangers, Chemical Engineering Research and Design 109 (2016) 628-637.

[55] T. Srinivas, A. Venu Vinod, Heat transfer intensification in a shell and helical coil heat exchanger using water-based nanofluids, Chemical Engineering and Processing: Process Intensification 102 (2016) 1-8.

[56] A. Alimoradi, M. Olfatia, M. Maghareh, Numerical investigation of heat transfer intensification in shell and helically coiled finned tube heat exchangers and design optimization, Chemical Engineering & Processing: Process Intensification 121 (2017) 125-143.

[57] H. Barzegari, A. Tavakoli, D. Jalali Vahid, Experimental study of heat transfer enhancement in a helical tube heat exchanger by alumina nanofluid as current flow, Heat Mass Transfer 55 (2019) 2679-2688.

[58] B.A. Kumar Naik, A.V. Vinod Heat transfer enhancement using non-Newtonian nanofluids in a shell and helical coil heat exchanger, Experimental Thermal and Fluid Science 90 (2018) 132-142.

[59] M.R. Salem, K.M. Elshazly, R.Y. Sakr, R.K. Ali, Experimental investigation of coil curvature effect on heat transfer and pressure drop characteristics of shell and coil heat exchanger, Journal of Thermal Science and Engineering Applications 7 (2015) 011005.

[60] A.F. Niwalkar, J.M. Kshirsagar, K. Kulkarni, Experimental investigation of heat transfer enhancement in shell and helically coiled tube heat exchanger using SiO_2/ water nanofluids, Materials Today Proceedings 18 (2019) 947-962.

[61] K. Palanisamy, P.C. Mukesh Kumar, Experimental investigation on convective heat transfer and pressure drop of cone helically coiled tube heat exchanger using carbon nanotubes/water nanofluids, Heliyon 5 (2019) e01705.

[62] P.J. Fule, B.A. Bhanvase, S.H. Sonawane, Experimental investigation of heat transfer enhancement in helical coil heat exchangers using water based CuO nanofluid, Advanced Powder Technology 28 (2017) 2288-2294.

[63] R. Andrzejczyk, T. Muszynski, Thermodynamic and geometrical characteristics of mixed convection heat transfer in the shell and coil tube heat exchanger with baffles, Applied Thermal Engineering 121 (2017) 115-125.

[64] J. Wang, S.S. Hashemi, S. Alahgholi, M. Mehri, M. Safarzadeh, A. Alimoradi, Analysis of Exergy and energy in shell and helically coiled finned tube heat

exchangers and design optimization, International Journal of Refrigeration 94 (2018) 11-23.

[65] A. Alimoradi, F. Veysi, Prediction of heat transfer coefficients of shell and coiled tube heat exchangers using numerical method and experimental validation, International Journal of Thermal Sciences 107 (2016) 196-208.

[66] M. Sepehr, S.S. Hashemi, M. Rahjoo,V. Farhangmehr, A. Alimoradi, Prediction of heat transfer, pressure drop andentropy generation in shell and helically coiledfinned tube heat exchangers, Chemical Engineering Research and Design 134 (2018) 277-291.

[67] A.S. Baqir, H.B. Mahood, A.R. Kareem, Optimisation and evaluation of NTU and effectiveness of a helical coil tube heat exchanger with air injection, Thermal Science and Engineering Progress 14 (2019) 100420.

[68] A. Alimoradi, Study of thermal effectiveness and its relation with NTU in shell and helically coiled tube heat exchangers, Case Studies in Thermal Engineering 9 (2017) 100-107.

[69] M. Zaboli, S.S.M. Ajarostaghi, M. Noorbakhsh, Effects of geometrical and operational parameters on heat transfer and fluid flow of three various water based nanofluids in a shell and coil tube heat exchanger, SN Applied Sciences 1 (2019) 1387.

Highlights

- A new modification for helically coiled heat exchanger.
- Numerical comparison with a conventional heat exchanger.
- Numerical analysis and experimental validation of the new modification.
- Average deviation among CFD and empirical findings is 8%.

Declaration of interests

☒ The authors declare that they have no known competing financial interests or personal relationships that could have appeared to influence the work reported in this paper.

☐The authors declare the following financial interests/personal relationships which may be considered as potential competing interests: